Research Square

Preprints are preliminary reports that have not undergone peer review.
They should not be considered conclusive, used to inform clinical practice,
or referenced by the media as validated information.

Rethink the subsistence of Pastoralists in the Middle Tian Shan: carbon and nitrogen isotopes evidence for the mixed subsistence in Wulasitai Valley, Xinjiang, 900BC – 1500 AD

Ying Zhang
Northwest University
Kangte He
University College London
Xiangpeng Zhang
Xinjiang Institute of Cultural Relics and Archaeology
Xiang Liu
liuxiangscofy@163.com

Northwest University

Research Article

Keywords:

Posted Date: March 2nd, 2026

DOI: https://doi.org/10.21203/rs.3.rs-8836084/v1

License: This work is licensed under a Creative Commons Attribution 4.0 International License. Read Full License

Additional Declarations: No competing interests reported.

Abstract

The Middle Tian Shan has often been characterised as a predominantly pastoral or nomadic zone during the Iron Age and historical periods, yet the role of agro-pastoral strategies in shaping subsistence practices in this mountainous region remains poorly understood. This study presents new carbon ($\delta^{13}C$) and nitrogen ($\delta^{15}N$) stable isotope data from human bone collagen recovered from the Wulasitai Valley in the central Tian Shan, China, spanning the Early Iron Age to the late historical period (ca. 900 BC–AD 1500).

The isotopic results indicate that subsistence in the Wulasitai Valley was consistently based on a mixed agro-pastoral economy, combining C_3 plant consumption with substantial intake of terrestrial animal protein, including meat and dairy products. While $\delta^{15}N$ values remain relatively stable through time, suggesting long-term continuity in animal protein consumption, $\delta^{13}C$ values fluctuate markedly, reflecting variable incorporation of C_4 plants, particularly millet. By integrating isotopic evidence with regional palaeoenvironmental data from the Bosten Lake basin and modern climatic proxies, this study demonstrates that climatic variability and environmental constraints played a critical role in shaping dietary strategies. These findings challenge simplified models of uniformly pastoral lifeways and highlight long-term subsistence flexibility and environmental adaptation within the Tian Shan Mountain Corridor.

1. Introduction

Previous carbon and nitrogen stable isotope research has primarily focused on several key research questions, including the trophic level, diet, and subsistence strategies of ancient populations; the domestication, dispersal, and adoption of crops; and the ways in which humans exploited and transformed natural landscapes (Lee-Thorp 2008). Particular attention has been paid to pastoral and nomadic subsistence systems (Murphy et al. 2013; Lightfoot et al. 2015; Hermes et al. 2018; Oleszczak et al. 2023), as well as to the timing and mechanisms of westward millet dispersal and eastward wheat and barley transmission. Central to these discussions is the role played by Central Asian pastoralists in mediating crop exchange and the processes by which millet and wheat were incorporated into regional subsistence regimes during the Bronze Age and Early Iron Age (Frachetti et al. 2010; Dodson et al. 2013; An et al. 2013; Betts et al. 2014; Zhou and Garvie-Lok 2015; Long et al. 2018; Hermes et al. 2019; Wang et al. 2019, 2023; Svyatko et al. 2021; Ventresca-Miller et al. 2023).

Within this broader framework, the Inner Asian Mountain Corridor (IAMC) has been widely recognised as a critical conduit for the dispersal of millet, barley, and wheat across Eurasia (Frachetti et al. 2010; Hermes et al. 2019). Notably, an increase in the consumption of C_4 plants—particularly millet—has been observed among steppe populations during the Late Bronze Age (ca. 1800–1500 BC), and in some regions extending into the so-called Final Bronze Age (ca. 1500–1000 BC) and Early Iron Age (after 1000 BC) (Lightfoot et al. 2015; Ananyevskaya et al. 2018). Similar trends have been documented in the Minusinsk Basin (Svyatko et al. 2021) and Tian Shan corridor (Matuzeviciute et al. 2022). However, Isotopic evidence from the southern Pamir Plateau indicates that Early Iron Age populations relied primarily on C_3 terrestrial plants and sheep-based pastoral economies, with limited consumption of C_4 crops (Guo et al. 2020), which shows the non-uniform of C_4 intake in this period.

Although millet is well adapted to semi-arid environments, its successful cultivation and sustained incorporation into agro-pastoral economies nonetheless depend on adequate water availability and favourable soil conditions (Ventresca-Miller et al. 2023). Previous studies have emphasised factors such as altitude and temperature as key variables influencing ancient choices between wheat/barley and millet cultivation (Wang et al. 2020a). However, diachronic investigations into whether long-term climatic variability shaped subsistence strategies in the Eurasian steppe–mountain interface remain limited.

Against this background, the present study examines dietary and subsistence practices in the Wulasitai Valley of the central Tian Shan (Xinjiang, China) from the Iron Age to the historical period (ca. 900 BC–AD 1500). By integrating carbon and nitrogen isotope data with regional palaeoenvironmental evidence, this research explores the environmental and socio-

economic drivers of long-term dietary change in this key mountain corridor, thereby providing new insights into the adaptive strategies of agro-pastoral communities in the Tian Shan Corridor.

1.1 The Tian Shan Corridor

The Tian Shan (see Fig. 1-a.) lies at the centre of the Eurasian landmass, extending from Central Asia in the west to China in the east, with a total length of over 2,500 km, of which more than 1,700 km lie within China. The mountains exhibit pronounced topographic variation, ranging from the highest summit, Mount Tomur (7,435.3 m), to the lowest point at Lake Ayding (− 154 m). Due to aspect-related climatic gradients, the northern and southern slopes differ markedly in temperature and moisture regimes (Hu 2004). Correspondingly, vegetation displays a clear altitudinal zonation, transitioning from desert to steppe, forest, alpine meadow, and glacier environments (Hu 2004). This complex geomorphology has generated considerable environmental diversity, shaping both ecological communities and human subsistence strategies (Tian et al. 2021; Wang et al. 2023, 2024).

As the eastern core of the Inner Asian Mountain Corridor (IAMC), the Tian Shan has served as a key conduit of interaction between western and eastern Eurasia since the Bronze Age (Frachetti 2012). Human movements, crop dispersal, and technological transmission all passed through this corridor, gradually forming an interconnected, trans-Eurasian cultural network. Recent archaeological discoveries demonstrate that C_3 crops originating in Southwest Asia—such as wheat and barley—and C_4 crops originating in East Asia—such as broomcorn and foxtail millet—were transmitted bidirectionally through the Inner Asian Mountain Corridor/Tian Shan corridor (Frachetti et al. 2010; Motuzaite Matuzeviciute et al. 2015; Hermes et al. 2019; Zhou et al. 2020; Matuzeviciute et al. 2022; Endo et al. 2023).

The spread of these crops inherently reflects population interaction, as plant dispersal implies the transmission of knowledge, practices, and social contacts across regions. These processes highlight the pivotal role of the Tian Shan in facilitating prehistoric exchange and underscore its significance as a nodal region in early Eurasian globalization.

1.2 Research sites

The Wulasitai River (Fig. 1-b) is located in the central Tian Shan Mountains, within Hejing County of the Bayingolin Mongol Autonomous Prefecture, Xinjiang Uygur Autonomous Region (Editorial Committee of Encyclopedia of Rivers and Lakes in China 2014). It occupies a strategically important position as a natural corridor linking the northern and southern slopes of the Tian Shan. To the north, the valley provides access toward the Urumqi region; to the east, it connects with the Turpan Basin via the Aragou corridor; to the south, it opens toward Bosten Lake and the Yanqi Basin; and to the west, it leads to the Dayouledusi Basin, also known as the Bayanbulak Grassland.

The Wulasitai Valley lies at elevations ranging from approximately 1,500 to 3,000 m and is characterised by a temperate continental climate, with a mean annual temperature of around 6°C and annual precipitation between 200 and 300 mm (Hong 1995, pp. 87–89). Owing to pronounced altitudinal gradients, soils in this mountainous region exhibit clear vertical zonation, and localised microclimatic variation strongly influences patterns of species diversity and distribution. Ecological surveys conducted on the southern slopes of the central Tian Shan demonstrate that the richness of seed plant families, genera, and species follows a unimodal pattern along the elevation gradient, increasing initially with altitude and then declining, with peak diversity occurring at elevations of approximately 1,900–2,000 m (Liu et al. 2018).

This region, in the prehistoric age, the pastoralists formed Chawuhu culture located here, which date to the Early Iron Age and roughly correspond to the Western Zhou to Warring States periods in the Central Plains. Chawuhu culture is located in the central Tianshan region of Xinjiang, with its core distribution in the Yanqi Basin (Xinjiang Uygur Autonomous Region Cultural Relics and Archaeology Institute 1999, 2016; Sun 2024). The population primarily comprised individuals of mixed European–East Asian ancestry (Xie et al. 2005; Li et al. 2025), and subsistence strategies were based on a combination of pastoralism and agriculture (Dong et al. 2022a). The Chawuhu culture is widely considered to have been influenced by the

Andronovo and post–Andronovo cultures (Wu 2023; Sun 2024), and maintained close cultural exchanges with various groups, including the Saka cultures of the eastern steppe (Cosmo 1996; Shulga et al. 2019; Ivanovich and Petrovich 2020). The three stages of this period in Wulasitai include the Early Stage (900 – 750), Middle stage (750 – 400 BC) and Late stage (400–100 BC, with some determinations possibly extending towards the turn of the Common Era), see (Gao et al. 2026, in press)

In historical periods, this region belonged to the ancient kingdom of *Yanqi (□□)*, as recorded in the *Hanshu* (*Book of Han □□*), "Account of the Western Regions." As early as 89 BC, the *Yanqi* came under the control of the Han Dynasty (Huang 1989). Following the establishment of the Protectorate of the Western Regions *(Xiyu Duhu □□□□)* by *Emperor Xuan (Han Xuandi□□□)* of the Western Han in 59 BC, Yanqi was placed under direct Han administration (Ban 1962, p. 3874). During the Eastern Han, the offices of the Protectorate of the Western Regions and temporary Commandery *(Wuji xiaowei □□□□)* were established in AD 74, and by AD 127 Yanqi was again incorporated into the jurisdiction of the Anxi Protectorate (Fan 1965, p. 2928).

Subsequently, the Yanqi Kingdom frequently maintained tributary and subordinate relations with successive Central Plains dynasties. It sent royal hostages to the *Cao Wei (□□)* in AD 227 and offered tribute to *Cao Wei* (AD 220, 240) and the *Western Jin dynasty (□□ AD 270)* (Chen 1964, pp. 58, 92; Fang 1974a, p. 13, b, p. 60). During the *Sixteen Kingdoms period (Shiliu Guo □ □□AD 304–439)*, the *Former Liang (□□ AD 301–376)* exerted direct control over *Yanqi* around AD 345, making it a vassal state (Fang 1974c). *Yanqi* subsequently submitted to Former Qin and Northern Wei authority (Fang 1974d; Li 1974).

With the rise of the Western Turkic Khaganate, *Yanqi* fell temporarily under Turkic influence, until it was formally incorporated into the Tang administrative system as part of the Anxi Protectorate *(Anxi Duhufu □□□□□)*, where a military garrison was established (Liu 1975, p. 1648; Wang 1991). Thereafter, control of the *Yanqi* region was contested among the *Tang dynasty (□ AD 618–907)*, the Tibetan Empire, and the Uyghur Khaganate. From the late Tang period until the arrival of the Yuan Dynasty in the 13th century, Yanqi was subordinated to the *Gaochang Uyghurs (□□□□)* and referred to as *Suolimi (□□ □)* (Geng and Zhang 2008). During the Yuan Dynasty, the region was designated as *Bashiboli (□□□□□)*(Liu 2006, p. 18). In the early Ming period, a polity known as the *Bieshibali* Kingdom *(□□□□□)*, also referred to as the Eastern Chagatai Khanate, was established, and the Ming court later renamed the region *Chalishi (□□□)* (Li 2012, pp. 26–27).

Historical sources further indicate that agriculture in the Yanqi Basin was highly developed during the *Western Han dynasty (□□206 BC–AD 8)*, with surplus grain production sufficient for export and storage in other states (Ban 1962, p. 3921). In AD 450, following an invasion and subsequent famine in the *Cheshi Kingdom (□□□)*, the *Northern Wei (□□ AD 386–535)* court opened grain reserves in Yanqi to provide relief (Fang 1974d, p. 3212). Crop diversity in Yanqi was considerable: the *Book of Wei* (*Weishu □□*) records that between the 4th century and late 6th century AD, Yanqi possessed a cold climate but fertile soils, producing rice, millet, legumes, and wheat (Wei 1974, p. 226). The *New Book of Tang (Xin Tangshu □□□)* notes that during the *Tang dynasty (□ AD 618–907)*, irrigation canals were used extensively and the land was suitable for millet and grape cultivation (Ouyang and Song 1975, p. 6228). By contrast, ethnographic investigations indicate that in more recent times millet cultivation survived only in limited areas of southern Xinjiang (Kuropatkin 1882, p. 34; Bellér-Hann 2008, p. 113).

The focus of this study is the Wulasitai cemetery and the Xiaxinguang cemetery and settlement, located on the southeastern bank of the Wulasitai Valley. In 2021, rescue excavations were conducted at these sites in advance of construction related to the Urumqi–Yuli Expressway (Hejing section).

This study applies carbon–nitrogen stable isotope analysis to human remains recovered from the Wulasitai cemetery and the Xiaxinguang site and cemetery, with the aim of reconstructing subsistence strategies in central Tian Shan from the Early Iron Age through to the historical period (cal. 900 BC–AD 1500). On this basis, the central Tian Shan—an important intersectional zone—is situated within the broader eastern Eurasian steppe context to allow systematic comparison of subsistence patterns across different ecological settings from the Bronze Age to the Iron Age. Further, this research seeks

to clarify the chronology of widespread adoption of C_3 and C_4 crops in the Tian Shan region and to explore the underlying factors that drove these transformations.

2. Materials and Methods

This study selected a total of 48 samples from the Wulasitai cemetery, the Xiaxinguang site, and the Daxigou site for radiocarbon dating. These samples include human bone and wood/charcoal materials. Of the total, 36 samples consist of well-preserved, dense human bones exhibiting minimal surface corrosion; nine samples derive from wooden grave structures; and three samples are charcoal recovered from a domestic context with clearly defined stratigraphy. Wood and charcoal samples were collected only when the outermost growth rings could be identified, thereby minimising the potential impact of the “old wood” effect.

2.1 Materials and their contexts

Early Iron Age (EIA, 900 – 100 BC)

During this phase, sixteen graves (M1–M16) were excavated at the Xiaxinguang site. Based on their construction, the burial features can be grouped into four types: square stone enclosures, square stone mounds, circular stone enclosures, and circular stone mounds. The tombs themselves comprise three structural forms: vertical pit stone-chamber tombs used for single interments, pouch-shaped stone-chamber tombs, and side-chamber tombs intended for collective or multiple burials. The number of individuals represented in each tomb ranges from two to more than twenty. The associated grave goods include bronze swords, bronze knives, bronze horse bits, gold rings, pottery jars, wooden artefacts, glass beads, and agate beads (Gao et al. 2026, in press). In addition, spouted jars recovered from the Wulasitai cemetery (Fig. 3) display diagnostic characteristics of the Chawuhu cultural tradition (Mingzhe and Enguo 1999; Wu 2022; Sun 2024) and are dated to 3000–2000 BP (see Sun 2024).

At the Xiaxinguang site, two large stone-built dwelling structures, designated Xiaxinguang F1 and F2, were excavated. Structure F1 occupies an area of approximately 100 m², whereas F2 covers about 239 m². Both dwellings yielded hearths, ash layers, burials, and a wide range of ceramic, bronze, iron, stone, and bone artefacts. Comparable evidence was obtained at the Daxigougoukou site, where excavations uncovered a large stone-constructed dwelling (2021XHDF1) with an area of roughly 175 m² (Gao et al. 2026, in press).

Historical periods (1-1500 AD)

A total of ten late-phase burials were subjected to radiocarbon dating in this study, including two from the Xiaxinguang cemetery and eight from the Wulasitai cemetery. Based on grave construction, these burials can be classified into three types: vertical pit graves, surface stone-cist graves, and vertical pit graves with lateral chambers. Both burials at Xiaxinguang belong to the vertical pit type. At Wulasitai, four burials are surface stone-cist graves and four are vertical pit graves with lateral chambers. All burials are single interments, and those with sufficiently preserved skeletal remains indicate extended supine inhumation.

Radiocarbon results indicate that Xiaxinguang burial M10 dates to the late 1st century BC to the early 2nd century AD, while M11-a dates to the mid-1st century AD to the early 3rd century AD. At Wulasitai, burial M1 dates to the mid-1st to early 3rd century AD; M17 to the mid-3rd to mid-4th century AD; M21 to the mid-3rd to late 4th century AD; M18 to the mid-3rd to early 5th century AD; and M5 to the early 5th to mid-6th century AD. Later burials include M8-1, dated to the late 9th to late 10th century AD; M8-2, dated to the late 9th to early 11th century AD; M7, dated to the late 13th to late 14th century AD; and M11, dated to the early 14th to middle 15th century AD.

When burial types is considered alongside chronological data, Xiaxinguang burials M10 and M11-a—both vertical pit graves—can be assigned broadly to the period from the late 1st century BC to the early 3rd century AD. At Wulasitai, burials M1,

M17, M21, M18, and M5 are surface stone-cist graves, with a long duration spanning from approximately the late 1st century BC to the mid-6th century AD. In contrast, burials M8-1, M8-2, M7, and M11 are vertical pit graves with lateral chambers and cluster chronologically between the late 9th century and the middle 15th century AD.

2.2 Methods

2.2.1 Materials and sampling

All samples used in this study consist of well-preserved human bones with no visible surface contamination, fractures, or fissures. In total, forty samples were collected and analysed. All human remains derive from chronologically well-defined burial contexts: twenty-eight samples belong to the Early Iron Age (ca. 900– 100 BC, see Gao et al., in press), and twelve samples come from historical-period contexts (ca. 1-1500 AD).

2.2.2 Collagen extraction

Collagen extraction was carried out at Lanzhou University following established protocols. Approximately 1 g of dense cortical bone was sectioned using an electric saw, after which the bone surfaces were polished and cleaned in an ultrasonic bath. The samples were subsequently demineralised in 0.5 M HCl and treated with 0.125 M NaOH to remove humic contaminants. They were then gelatinised in weakly acidic solution (pH 3) at 75°C for 48 hours. The resulting gelatin solution was filtered through a pre-cleaned filter tube, frozen, stored at 4°C for two days, and finally freeze-dried in a lyophiliser to obtain purified collagen.

2.2.3 Carbon and nitrogen isotopes test

Carbon and nitrogen isotope compositions were measured using an Isoprime precisION IRMS at the Zhinanzhen Laboratory. International and laboratory standards (B2159 and USGS61) were used for calibration, and every batch of ten samples included a duplicate measurement of one sample to ensure instrumental precision. Results from repeated measurements of the standards indicate that analytical errors for both $\delta^{13}C$ and $\delta^{15}N$ were less than ± 0.2‰. The stable isotope ratio results were analyzed as the ratio of the heavier isotope to the lighter isotope (13C/12C or 15N/14N) and reported as δ in parts per 1,000 or “per mil (‰)”, e. δ13C (δ15N) = 1000 × [(Rsamples/Rstandard)-1], where Rsample and Rstandarad are the 13C/12C and 15N/14N, relative to the internationally defined standards for carbon (VPDB, Vienna Pee Dee Belemnite) and nitrogen (AIR, Ambient Inhalable Reservoir) (see Coplen 2011).

2.2.4 Radiocarbon dating

The testing includes three main steps: pretreatment, graphitisation, and Accelerator Mass Spectrometer (AMS) testing, which details are referred to in Cao et al. (2023). All testing was processed by the radiocarbon laboratory of Lanzhou University. In the pretreatment step, samples were treated with an acid solution, an alkaline solution and an acid solution again to remove carbonates, humic acids and the carbonate precipitate that may have been generated due to the reaction with atmospheric CO2 during the alkali reaction and again rinsing the sample with Milli-Q water to achieve neutral pH. For bone samples, after the process mentioned before, the samples were reacted in an acid solution and frozen to complete the collagen extraction process. All details can be found in the supplementary materials. Calibrated Radiocarbon ages were calculated by the IntCal20 calibration curve (Reimer et al. 2020) from the online program OxCal (Ramsey 2009, 2021).

2.2.5 Environmental analysis

Environmental change has long been recognised as a potential driver of subsistence transformation in Central Asia and the Tian Shan, yet few studies have explicitly integrated palaeoenvironmental data into diachronic discussions of subsistence strategies. In the Discussion section, Section 3.1 therefore combines palaeoenvironmental records from Bosten Lake with isotopic evidence from the Wulasitai Valley to examine long-term changes in human subsistence and their potential environmental drivers. The palaeoenvironmental datasets employed derive primarily from published sedimentary, palynological, and geochemical studies of Bosten Lake (Zhong and Xiong 1998; Huang et al. 2009, 2010, 2021, 2023; Li et

al. 2020; Xiang et al. 2021; Zheng et al. 2025), which provide high-resolution reconstructions of hydroclimatic variability in the eastern Tian Shan.

Section 3.2 further contextualises the Wulasitai results through comparison with published isotopic datasets spanning the Early Iron Age to the Medieval period. In Section 4.2, discussed sites are grouped into four chronological clusters—Early Iron Age I (EIA-I, ca. 1000–600 BC), Early Iron Age II (EIA-II, ca. 700–300 BC), Early Iron Age III (EIA-III, ca. 400 BC–AD 1) and historical period (after AD 1)—allowing for limited chronological overlap. This clustering facilitates examination of diachronic trends while also considering the influence of geographic and topographic variability. Previous research has suggested that $\delta^{13}C$ distributions reflect the relative availability of wheat/barley and millet, which in turn is closely linked to the vertical zonation of the Tian Shan landscape and elevation-dependent environmental constraints (Wang et al. 2020a). Crop cultivation is further conditioned by temperature, solar radiation, water availability, and soil fertility.

To evaluate the role of environmental constraints without attempting a direct reconstruction of past climate conditions, modern environmental variables were employed as proxies for long-term landscape controls (cf. D'Alpoim Guedes and Butler 2014; Ventresca-Miller et al. 2023), under the assumption that broad climatic gradients and topographic controls have remained relatively stable throughout the mid-to-late Holocene. By linking human $\delta^{13}C$ values to modern climatic and landscape gradients, this study assesses how environmental factors may have structured the adoption and intensity of C_3 and C_4 plant use.

Given that millet generally requires temperatures above 10°C for effective germination(Kamkar et al. 2006), whereas wheat can germinate at much lower temperatures (1–2°C; Porter and Gawith 1999), and that millet has substantially lower water requirements than wheat (Mekonnen and Hoekstra 2011, p. 1585), two climatic variables were selected as key constraints on crop growth: the Number of Growing Degree Days above 10°C (NGD10) and the Accumulated Precipitation on Growing Season Days (GSP), see Brun et al. (2022a, b). These variables were obtained from the CHELSA climate dataset (https://www.chelsa-climate.org/datasets/chelsa_bioclim; see Supplementary Material named CN isotopes dataset).

Statistical analyses were conducted to assess relationships between environmental variables and $\delta^{13}C$ values. Linear regression models were applied, and Pearson's correlation coefficients were calculated to quantify linear associations between variables. In addition, Spearman's rank correlation coefficients were used to evaluate monotonic relationships without assuming normal data distributions. All statistical analyses were performed using R version 4.5.2.

3. Results

3.1 The condition of samples

Based on the results of isotope ratio mass spectrometry, the collagen extracted from human bone samples exhibits carbon and nitrogen contents ranging from 41.81% to 43.21% and 15.19% to 15.87% by weight, respectively. The atomic carbon-to-nitrogen (C: N) ratios of these samples fall between 3.17 and 3.22 (Table 1), which lies within the accepted range of 2.9 to 3.6 for well-preserved collagen (DeNiro 1985; Ambrose 1990) suitable for AMS radiocarbon dating and C N isotope analysis.

3.2 Radiocarbon dates

Based on the radiocarbon chronology (Fig. 3 and Table 1), the archaeological remains of the Wulasitai Valley can be divided into seven stages. Each stage is characterised by distinct burial forms and grave-good assemblages, reflecting changes in material culture over time. The Early Iron Age sequence can be further subdivided into three phases: an Early Stage (cal. 900–750 BC), a Middle Stage (cal. 750–400 BC), and a Late Stage (cal. 400–100 BC, extending slightly across the BC/AD boundary). Throughout these three phases, burials are dominated by vertical pit stone-chamber tombs for single individuals and pouch-shaped stone-chamber tombs. Ceramic assemblages commonly include spouted jars, which are diagnostic

artefacts of the Chawuhu cultural tradition. Detailed chronological distinctions and specific mortuary practices associated with these Early Iron Age phases are discussed elsewhere (Gao et al. 2026, in press).

With the transition into the historical period, stone-chamber tombs disappear and are replaced by surface stone-cist graves and vertical pit earth graves. Ceramic vessels are no longer included as grave goods. On the basis of radiocarbon dates, these historical-period burials can be divided into four stages. The first stage corresponds to the Eastern Han and Xiongnu period (Yanqi Kingdom; cal. AD 1–200). The second stage dates to the Wei–Jin and Northern–Southern Dynasties period (cal. AD 250–550). Burials from these two stages typically contain very limited grave goods, mainly small ornaments.

The third stage corresponds to the Late Tang–Five Dynasties period through the early Northern Song (cal. AD 890–1050). Graves from this phase yielded artefacts associated with horse equipment, high-value gilt textiles, and characteristic Central Plains Tang-period bronze mirrors decorated with sea-creature and grapevine motifs. The fourth stage dates to the Yuan Dynasty through the early Ming period (cal. AD 1250–1450), and is characterised by the presence of iron stirrups and Central Plains–style bronze mirrors depicting narrative scenes typical of the Yuan (AD 1206–1368) –Ming (AD 1368–1644) dynasty.

Together, these shifts in burial practice and associated material culture document long-term transformations in social organisation, external connectivity, and cultural affiliation in the Wulasitai Valley from the Early Iron Age through the historical period.

Table 1

CN isotope results and AMS ^{14}C results from burials and dwellings at Xiaxinguang (X), Wulasitai (W), and Daxigougoukou (D). In this table, “F” and “M” denote contexts identified as dwellings and graves, respectively. Combined contexts are represented as “F_M”; for example, “F2_M3” refers to grave M3 located within dwelling F2. “F_L” indicates stratigraphic layers within dwellings—for instance, “F2_L3” denotes the third layer of dwelling F2—while “M3_L2” refers to the second stratigraphic layer of grave M3. Surface layers are designated as “L1”, with deeper layers numbered sequentially (e.g., L2 beneath L1). In addition, “F1_ZD10”, “F1_K3”, and “F1_HD1L3” refer to posthole D10, pit K3, and the third layer of pit HD1 within dwelling F1, respectively. Superscript symbols indicate samples derived from the same dwelling or burial context

Lab. No.	Site	Context	Material	Skeletal element	14C date (BP)	Modelled cal. date (2σ)	δ13C (‰)	δ15N (‰)	Stage	Ref.
LZU24329	X	M10_L1	Human bone	Phalange	1966 ± 21	19AD-123AD	-17.7	10.8	Historical Stage I	This study
LZU24306	W	M1	Human bone	Phalange	1933 ± 24	24AD-154AD	-17.8	12.1	Historical Stage I	This study
LZU24330	X	M11_L1	Human bone	Rib	1918 ± 19	30AD-198AD	-17.4	11.7	Historical Stage I	This study
LZU24313	W	M17	Human bone	Phalange	1774 ± 24	232AD-360AD	-17.6	11.5	Historical Stage II	This study
LZU24315	W	M21	Human bone	Rib	1749 ± 21	246AD-377AD	-18.1	11.9	Historical Stage II	This study
LZU24314	W	M18	Human bone	skull	1729 ± 24	252AD-406AD	-18.4	12.0	Historical Stage II	This study
LZU24307	W	M5	Human bone	Rib	1594 ± 25	325AD-552AD	-18.8	12.1	Historical Stage II	This study
LZU24309	W	M8[10]	Human bone	Rib	1109 ± 27	895AD-995AD	-17.0	12.9	Historical Stage III	This study
LZU24344	W	M9	wood		1105 ± 18	895AD-995AD			Historical Stage III	This study
LZU24343	W	M8[10]	wood		1103 ± 18	894AD-995AD			Historical Stage III	This study
LZU24310	W	M8[10]	Human bone	Rib	1051 ± 24	898AD-1025AD	-16.7	12.1	Historical Stage III	This study
LZU24308	W	M7	Human bone	Rib	656 ± 22	1284AD-1395AD	-17.3	11.5	Historical Stage IV	This study
LZU24342	W	M6	wood		578 ± 17	1318AD-1410AD			Historical Stage IV	This study
LZU24311	W	M11	Human bone	Rib	551 ± 22	1321AD-1425AD	-18.1	10.9	Historical Stage IV	This study
LZU24338	X	F2_M3[1]	Human bone	Rib	2719 ± 26	879–803 BC	-19.0	12.6	Early Stage	(Gao et al. 2026, in press)
LZU24316	W	M25	Human bone	Rib	2688 ± 22	891–801	-18.4	12.0	Early Stage	(Gao et al. 2026, in press)

Lab. No.	Site	Context	Material	Skeletal element	14C date (BP)	Modelled cal. date (2σ)	δ13C (‰)	δ15N (‰)	Stage	Ref.
LZU24351	X	F1_L7[2]	Charcoal	–	2676 ± 20	840–798			Early Stage	(Gao et al. 2026, in press)
LZU24317	W	M26	Human bone	Rib	2650 ± 22	830–795	-18.3	12.2	Early Stage	(Gao et al. 2026, in press)
LZU24339	X	F1_M2[2]	Human bone	Rib	2629 ± 25	828–789	-18.1	14.7	Early Stage	(Gao et al. 2026, in press)
LZU24337	X	F2_L3[1]	Human bone	Limb	2511 ± 26	775–544	-18.4	12.3	Middle Stage	(Gao et al. 2026, in press)
LZU24340	X	F1_M6[2]	Human bone	Limb	2498 ± 26	771–543	-19.1	12.7	Middle Stage	(Gao et al. 2026, in press)
LZU24349	X	F1_L8[2]	Charcoal	–	2466 ± 20	758–516			Middle Stage	(Gao et al. 2026, in press)
LZU24312	W	M12_L3	Human bone	Rib	2445 ± 26	520–413	-19.1	13.1	Middle Stage	(Gao et al. 2026, in press)
LZU24327	X	M8	Human bone	Rib	2429 ± 21	518–413	-17.9	11.9	Middle Stage	(Gao et al. 2026, in press)
LZU24346	X	M2_L1[3]	Wood	–	2429 ± 19	517–413			Middle Stage	(Gao et al. 2026, in press)
LZU24347	X	M3_L2[4]	Wood	–	2428 ± 19	517–413			Middle Stage	(Gao et al. 2026, in press)
LZU24325	X	M6	Human bone	Rib	2424 ± 25	518–412	-18.1	12.1	Middle Stage	(Gao et al. 2026,

Lab. No.	Site	Context	Material	Skeletal element	14C date (BP)	Modelled cal. date (2σ)	δ13C (‰)	δ15N (‰)	Stage	Ref.
										in press)
LZU24353	D	F1_ZD10[5]	Wood	–	2418 ± 20	517–412			Middle Stage	(Gao et al. 2026, in press)
LZU24341	X	F1_M8[2]	Human bone	Rib	2417 ± 25	517–412	-19.3	4.6	Middle Stage	(Gao et al. 2026, in press)
LZU24321	X	M2_L3[3]	Human bone	Rib	2403 ± 26	515–411	-18.4	12.0	Middle Stage	(Gao et al. 2026, in press)
LZU24326	X	M7	Human bone	Rib	2402 ± 26	515–411	-18.2	11.4	Middle Stage	(Gao et al. 2026, in press)
LZU24354	D	F1_K3[5]	Wood	–	2388 ± 20	513–409			Middle Stage	(Gao et al. 2026, in press)
LZU24322	X	M3_L2[4]	Human bone	Ulna	2384 ± 25	514–409	-18.6	13.4	Middle Stage	(Gao et al. 2026, in press)
LZU24345	X	M1_L2[6]	Wood	–	2336 ± 19	406–380			Late Satge	(Gao et al. 2026, in press)
LZU24333	X	M13_L2	Human bone	Rib	2330 ± 19	405–379	-18.0	12.5	Late Satge	(Gao et al. 2026, in press)
LZU24331	X	M12_L1[7]	Human bone	Rib	2285 ± 19	397–367	-18.1	12.6	Late Satge	(Gao et al. 2026, in press)
LZU24318	X	M1_L1[6]	Human bone	Rib	2268 ± 22	395–362	-18.3	12.6	Late Satge	(Gao et al. 2026, in press)

Lab. No.	Site	Context	Material	Skeletal element	14C date (BP)	Modelled cal. date (2σ)	δ13C (‰)	δ15N (‰)	Stage	Ref.
LZU24352	D	F1_L3[5]	Charcoal	–	2267 ± 21	396–361			Late Satge	(Gao et al. 2026, in press)
LZU24336	X	M15_L1[8]	Human bone	Rib	2266 ± 25	396–361	-18.3	12.3	Late Satge	(Gao et al. 2026, in press)
LZU24335	X	M14_L3[9]	Human bone	Metatarsal	2265 ± 25	396–362	-18.1	12.1	Late Satge	(Gao et al. 2026, in press)
LZU24348	X	M15_L1[8]	Wood	–	2256 ± 19	394–362			Late Satge	(Gao et al. 2026, in press)
LZU24332	X	M12_L3[7]	Human bone	Rib	2232 ± 19	371–201	-17.7	12.7	Late Satge	(Gao et al. 2026, in press)
LZU24323	X	M4	Human bone	Rib	2213 ± 28	363–176	-16.9	12.6	Late Satge	(Gao et al. 2026, in press)
LZU24319	X	M1_L2[6]	Human bone	Rib	2201 ± 21	356–176	-18.4	5.7	Late Satge	(Gao et al. 2026, in press)
LZU24328	X	M9_L1	Human bone	Phalange	2196 ± 23	355–173	-17.5	12.7	Late Satge	(Gao et al. 2026, in press)
LZU24324	X	M5_L2	Human bone	Phalange	2195 ± 25	355–172	-17.8	12.7	Late Satge	(Gao et al. 2026, in press)
LZU24320	X	M2_L1[3]	Human bone	Rib	2152 ± 25	351–101	-16.6	12.5	Late Satge	(Gao et al. 2026, in press)
LZU24334	X	M14_L1[9]	Human bone	Rib	2068 ± 25	344–1	-16.7	16.1	Late Satge	(Gao et al. 2026,

Lab. No.	Site	Context	Material	Skeletal element	14C date (BP)	Modelled cal. date (2σ)	δ13C (‰)	δ15N (‰)	Stage	Ref.
										in press)

3.3 Results of C, N isotopes

This study conducted radiocarbon dating on human remains, charcoal, and wood samples recovered from three sites—Wulasitai, Xiaxinguang, and Daxigoukou. The results indicate that the cultural sequence of the Wulasitai Valley from the Iron Age through the historical period can be divided into seven phases: three Early Iron Age stages (Early, Middle, and Late) and four historical stages (Historical Stages I–IV). Within this chronological framework, carbon and nitrogen stable isotope analyses were carried out on the dated human skeletal samples.

The results show that $\delta^{13}C$ values of human bone collagen from the Wulasitai Valley, spanning the Iron Age to the historical period, range from − 19.3‰ to − 16.6‰ (mean − 18.1‰), while $\delta^{15}N$ values range from 4.6‰ to 16.1‰ (mean 12.1‰). In general, populations subsisting primarily on C_3-based diets (e.g., wheat, barley, and herbivore-derived products) exhibit more negative $\delta^{13}C$ values, typically between − 22‰ and − 18‰, whereas values around − 12‰ reflect predominantly C_4-based diets. Values between − 12‰ and − 18‰ indicate mixed C_3/C_4 consumption, while values below − 18‰ suggest a largely C_3-based dietary regime (Ambrose and DeNiro 1986; Pechenkina et al. 2005; Barton et al. 2009; Wang et al. 2019).

Published isotopic data for herbivorous fauna in Xinjiang indicate $\delta^{15}N$ values ranging from 2.5‰ to 13.4‰ (n = 234; mean = 7.21‰, see the black error bar in Fig. 4, data from Chen et al. 2017a; Guo et al. 2020; Dong 2021; Dong et al. 2021). Given that $\delta^{15}N$ values typically increase by approximately 2–6‰ with each trophic level (Bocherens and Drucker 2003; McCutchan Jr et al. 2003; Hedges and Reynard 2007; O'Connell et al. 2012), these data suggest that most populations in the Wulasitai Valley relied on animal-derived protein, including meat and dairy products. In addition, two individuals exhibit isotopic signatures indicating little to no consumption of animal-derived protein (samples LZU24341 and LZU24319, which lower than 6‰, discussed in section 4.1). At the same time, carbon isotope values indicate that C_4 plants contributed variably to human diets, while some individuals primarily consumed mixed C_3/C_4 plant resources.

More specifically, individuals from the Early Stage of the Early Iron Age (n = 4) exhibit $\delta^{13}C$ values ranging from − 19.0‰ to − 18.1‰ (mean − 18.5‰) and $\delta^{15}N$ values from 12.0‰ to 14.7‰ (mean 12.9‰). Middle Stage Early Iron Age individuals (n = 9) show $\delta^{13}C$ values between − 19.3‰ and − 17.9‰ (mean − 18.6‰) and $\delta^{15}N$ values between 4.6‰ and 11.4‰ (mean 11.5‰). This pattern indicates a dietary regime dominated by C_3 plants and animal protein. Notably, one juvenile individual from Xiaxinguang dwelling F1, burial M8 (sample LZU24341; $\delta^{15}N$ = 4.6‰), shows minimal evidence for meat consumption.

During the Late Stage of the Early Iron Age, individuals (n = 12) display $\delta^{13}C$ values from − 18.3‰ to − 16.6‰ (mean − 17.7‰) and $\delta^{15}N$ values from 5.7‰ to 16.1‰ (mean 12.3‰). The slightly elevated $\delta^{13}C$ values indicate an increased contribution of C_4 plants during this phase, while overall levels of animal protein consumption remain broadly consistent. The highest $\delta^{15}N$ value (16.1‰) was recorded in an individual from burial M14L2 at the Xiaxinguang cemetery (sample LZU24334), who also exhibits a $\delta^{13}C$ value of − 16.7‰. This isotopic combination suggests a high trophic position, reflecting substantial consumption of terrestrial meat and dairy products rather than freshwater resources. The most positive $\delta^{13}C$ value (− 16.6‰) occurs in another Late Iron Age individual from the first layer of burial M2 at Xiaxinguang (sample LZU24320; $\delta^{15}N$ = 12.5‰), indicating a notable dietary contribution from C_4 plants. Similarly, one individual from the second layer of burial M2 (sample LZU24319; $\delta^{15}N$ = 5.7‰) appears to have consumed little animal protein.

For the historical periods, $\delta^{13}C$ values range from − 17.8‰ to − 17.4‰ (mean − 17.6‰) and $\delta^{15}N$ values from 10.8‰ to 12.1‰ (mean 11.5‰) in Historical Stage I (n = 3); from − 18.8‰ to − 17.6‰ (mean − 18.2‰) and 11.5‰ to 12.1‰ (mean 11.9‰) in Historical Stage II (n = 4); from − 17.0‰ to − 16.7‰ (mean − 16.9‰) and 12.1‰ to 12.9‰ (mean 12.5‰) in

Historical Stage III (n = 2); and from − 18.1‰ to − 17.3‰ (mean − 17.7‰) and 10.9‰ to 11.5‰ (mean 11.2‰) in Historical Stage IV (n = 2).

Overall, these results indicate no statistically significant difference in $\delta^{15}N$ values between Iron Age and historical populations in the Wulasitai Valley, suggesting that access to animal protein—including meat and dairy—remained relatively stable over the long term. In contrast, $\delta^{13}C$ values exhibit noticeable fluctuations through time, reflecting changes in the relative contribution of C_4 plants to human diets. This study will further examine whether these fluctuations are linked to environmental change and will situate the Wulasitai Valley within a broader comparative framework encompassing contemporaneous pastoral and agro-pastoral populations across the eastern Eurasian steppe–mountain zone.

4. Discussion

4.1 Subsistence in the Wulasitai valley

Carbon and nitrogen stable isotope data indicate that subsistence strategies in the Wulasitai Valley were primarily based on C_3 plants in combination with animal-derived protein, including meat and dairy products, while a subset of individuals also consumed mixed C_3/C_4 plant resources. Notably, two Early Iron Age individuals (samples LZU24341 and LZU24319) exhibit $\delta^{15}N$ values below 6‰, a pattern that requires careful interpretation.

Published $\delta^{15}N$ values for herbivorous fauna (cattle, sheep, and horses) in the Tian Shan region of Xinjiang range from ranging from 2.5‰ to 13.4‰ (n = 234; mean = 7.21‰, see the black error bar in Figure 4, data from Chen et al. 2017a; Guo et al. 2020; Dong 2021; Dong et al. 2021). Low $\delta^{15}N$ values in human collagen have also been documented at the Late Bronze Age site of Liushugou in the central Tian Shan, where two individuals ($\delta^{15}N$ = 6.2‰ and 7.1‰) were interpreted as representing groups with distinct dietary practices, possibly reflecting population movement or cultural heterogeneity (Dong et al. 2021). Similarly, at the Late Bronze Age site of Lisakovsk in Kazakhstan, six individuals yielded $\delta^{15}N$ values between 4.61‰ and 8.75‰ (Ventresca-Miller et al. 2023), suggesting that such low values may reflect post-depositional contamination or diagenetic alteration. However, this explanation appears insufficient, as other individuals from Lisakovsk also exhibit $\delta^{15}N$ values below 10‰ while maintaining C:N ratios within the accepted range for well-preserved collagen, indicating that the isotopic signatures are likely original rather than diagenetic.

Comparable low $\delta^{15}N$ values (around 5‰) have been observed in Early Holocene individuals from sites such as Lapa do Santo in Brazil, where diets were almost entirely plant-based and dominated by C_3 resources (Strauss et al. 2016). Likewise, Classic-period Maya populations in the lowlands and prehistoric groups in the Andean highlands—both largely reliant on plant-based diets—exhibit relatively low $\delta^{15}N$ values; Maya commoners, for example, typically show bone-collagen $\delta^{15}N$ values of approximately 6–8‰ (Schoeninger et al. 1983). In northern China, agricultural populations from the Neolithic through the Early Iron Age, whose subsistence depended primarily on C_4 crops, frequently exhibit $\delta^{15}N$ values below 6‰ (see Hu et al. 2006; Ma et al. 2016; Chen et al. 2017a).

Previous studies have generally characterised Bronze and Early Iron Age populations in the central Tian Shan as predominantly pastoral or agro-pastoral, with substantial reliance on C_4 plants and terrestrial animal products such as cattle and sheep (Guo et al. 2020; Wang et al. 2020b; Dong et al. 2021, 2022a; Li 2021; Dai et al. 2025). The isotopic evidence from Wulasitai—particularly the presence of individuals exhibiting very low $\delta^{15}N$ values—therefore complicates and challenges simplified models that portray Early Iron Age subsistence in this region as uniformly pastoral or nomadic.

This study proposes that such dietary variability is closely linked to environmental fluctuations between ca. 700 and 200 BC. To further evaluate the relationship between environmental change and subsistence strategies in the Wulasitai Valley, high-resolution palaeoenvironmental records from nearby Bosten Lake were incorporated into the analysis. Owing to its proximity to the study area, sedimentary sequences from Bosten Lake provide an effective proxy for reconstructing regional environmental dynamics. This study draws on multiple palaeoenvironmental indicators (Figure 5), including pollen A/C

ratios (Artemisia/Chenopodiaceae), grain-size distributions (μm), *Pediastrum* concentrations (coenobia/g), carbonate content (%), and carbonate $\delta^{18}O$ values (VPDB, ‰) (Zhong and Xiong 1998; Huang et al. 2009, 2023; Wang et al. 2020c; Xiang et al. 2021; Zheng et al. 2025). Together, these proxies allow for a detailed assessment of hydroclimatic variability and its potential influence on subsistence choices in the Middle Tian Shan during the late first millennium BC.

The pollen A/C ratio is particularly informative, as *Artemisia* prefers relatively humid steppe and meadow environments and responds sensitively to increased precipitation, whereas Chenopodiaceae are drought- and salt-tolerant taxa that dominate desert and extremely arid landscapes. Consequently, higher A/C ratios correlate positively with increased moisture availability and are widely used as effective indicators of humidity variation in arid and semi-arid regions (Xu et al. 2007; Huang et al. 2010; Wang et al. 2020c).

Grain-size distributions reflect sedimentary energy conditions: coarse fractions (sand and coarse silt) indicate strong winds, high hydrodynamic energy, low lake levels, or exposed surfaces, whereas fine fractions (fine silt and clay) reflect low-energy environments such as deeper or more stable water bodies (Huang et al. 2009; Schillereff et al. 2014). *Pediastrum*, a freshwater green alga, is highly sensitive to salinity and alkalinity; its abundance declines sharply when lake salinity exceeds approximately 2–3 g/L. High *Pediastrum* concentrations therefore indicate fresher water, higher lake levels, and increased effective moisture, whereas low or absent concentrations signal salinisation, falling lake levels, and arid conditions (Xiang et al. 2021; Huang et al. 2023). Carbonate content increases under enhanced evaporation and arid conditions, reflecting lake-water concentration, whereas lower values indicate dilution through increased precipitation or inflow (Deocampo 2010; Gierlowski-Kordesch 2010). Carbonate $\delta^{18}O$ values provide further insight into hydrological balance and climate: higher values reflect aridity and intensified evaporation, while lower values indicate more humid conditions and increased precipitation (Talbot 1990; Leng and Marshall 2004).

Previous studies indicate that Bosten Lake lies within a climatic regime dominated by the mid-latitude westerlies and characterised by long-term oscillations between warm–dry and cool–wet conditions (Zhong and Xiong 1998; Wünnemann et al. 2006; Chen et al. 2006; Huang et al. 2009, 2010; Xie et al. 2021). Against this background, palaeoenvironmental records suggest that between ca. 900 and 100 BC, although relatively low pollen A/C ratios, carbonate content, and $\delta^{18}O$ values generally point to warm and humid conditions, pronounced fluctuations in Pediastrum abundance, grain-size distributions, carbonate content, and $\delta^{18}O$ values indicate a highly unstable climate regime (Figure 5; see also (Figure 5; see also Wünnemann et al. 2006).

Around ca. 400–150 BC, Pediastrum concentrations reached pronounced minima, likely reflecting short-lived arid episodes (Chen et al. 2006, p. 105). Such episodes may have disrupted pastoral productivity by reducing pasture quality and water availability, thereby forcing local communities to rely more heavily on cultivated crops. These adaptive responses provide a plausible explanation for the emergence of individuals with unusually low $\delta^{15}N$ values at Wulasitai, reflecting reduced intake of animal-derived protein.

Around ca. 300 BC, carbonate content and $\delta^{18}O$ values reached minor peaks, signalling cooler and drier conditions, before declining again. During this interval, $\delta^{13}C$ values at Wulasitai increase markedly, indicating enhanced consumption of C_4 plants. This pattern suggests that deteriorating local environmental conditions constrained agricultural productivity and favoured the adoption of millet, a crop requiring comparatively less water. In terms of absolute crop water use and irrigation demand, millet is widely recognised as a drought-tolerant, low-water-demand crop, requiring less evapotranspiration and significantly less blue-water input than wheat and barley (Mekonnen and Hoekstra 2011, p. 1585) Consequently, under conditions of reduced precipitation and increasing aridity, millet would have represented a more resilient subsistence option. In addition, some C_4 crops may have been acquired through exchange with lower-altitude or plains-based communities.

Between AD 100 and 500, decreases in grain size, carbonate content, and $\delta^{18}O$ values, together with rising pollen A/C ratios, indicate a return to more humid conditions and a contraction of desert environments. These conditions would have

favoured local cultivation and a renewed emphasis on C_3 crops, consistent with the isotopic evidence from Wulasitai.

During the period ca. AD 750–1450, broadly overlapping with the Medieval Climate Anomaly (ca. AD 900–1350) and the onset of the Little Ice Age (ca. AD 1400-1700; see Mann et al. 2009; Graham et al. 2011), pollen A/C ratios declined sharply while Chenopodiaceae increased, and multiple environmental proxies indicate reduced humidity and the expansion of desert landscapes. Although declining $\delta^{18}O$ values may suggest higher temperatures, effective moisture likely decreased as a result of reduced precipitation (Xie et al. 2021, p. 9). Under such increasingly arid conditions, a higher reliance on C_4 plants—reflected in elevated $\delta^{13}C$ values—may have resulted from shifts in agricultural production and consumption driven by declining rainfall.

In this context, a mixed C_3–C_4 dietary strategy based on millet and wheat/barley would have helped mitigate the growing uncertainty associated with environmental change, thereby enhancing economic resilience (e.g., Ananyevskaya et al. 2018; Wilkin et al. 2020; Riccomi et al. 2020; Bleasdale et al. 2020; Ventresca-Miller et al. 2023). Benefiting from the arid conditions of Xinjiang, some foodstuffs were preserved in dried or dehydrated forms, providing direct archaeological evidence for such mixed subsistence practices. At the Beifang cemetery in the Tarim Basin (cal. 1550 BC), millet-based foods combined with wheat were identified (Xie et al. 2014). Similar millet–wheat food remains were recovered from the Subeixi cemetery in the Turpan Basin (ca. 350 BC; Shevchenko et al. 2014). At the Asitana cemetery dating to the Tang dynasty (AD 618–907), both foxtail millet and millet–wheat products were found (Chen et al. 2012). Notably, this mixed dietary tradition persisted into the early twentieth century. Ethnographic sources indicate that both millet and wheat were cultivated in the Tian Shan region at that time, supplemented by the acquisition of grains grown elsewhere through trade and exchange (e.g., Kuropatkin 1882, p. 186). Together, these lines of evidence suggest a long-term developmental trend from more specialized subsistence regimes toward increasingly flexible C_3–C_4 mixed dietary strategies.

Taken together, these data indicate that climatic variability was a key driver of long-term dietary change in the Wulasitai Valley. The observed flexibility in subsistence practices highlights the adaptive capacity of mountain agro-pastoral communities in the central Tian Shan, enabling them to respond effectively to environmental stress and increasing resource instability.

4.2 Long-term dynamics of wheat/barley and millet

Although the earliest evidence for the westward dispersal of C_4 crops—particularly broomcorn and foxtail millet—derives from the Tian Shan region and dates to the later third millennium BC (Frachetti et al. 2010), corresponding to the Early or Middle Bronze Age, previous carbon and nitrogen isotope studies indicate that C_3/C_4-mixed dietary did not become a major component of pastoralist diets until Final Bronze Age (~1400-1000 BC) and Early Iron Age (after 1000 BC) (Lightfoot et al. 2015; Motuzaite Matuzeviciute et al. 2015; Ananyevskaya et al. 2018; Li 2021; Svyatko et al. 2021; Matuzeviciute et al. 2022; Ventresca-Miller et al. 2023). Rising $\delta^{13}C$ values reflecting increased C_4 plant consumption have been documented across a wide geographical range, including the central Tian Shan of Xinjiang, northern, southern (western Tian Shan), and central Kazakhstan, the Minusinsk Basin of southern Siberia, and the Mongolian Altai. During the first millennium BC (Early Iron Age), mixed C_3/C_4 diets continued to characterise many nomadic populations in these regions (Lightfoot et al. 2015; Hermes et al. 2019; Wang et al. 2019; Svyatko et al. 2021; Matuzeviciute et al. 2022; Ventresca-Miller et al. 2023).

However, despite the widespread availability of C_4 crops across the western steppe zone by the Late Bronze Age, not all nomadic or agro-pastoral communities in the Tian Shan mountains and adjacent foothill regions fully adopted mixed C_3/C_4 subsistence strategies. This pattern is evident at a range of sites, including Mohuchahan in the central Tian Shan (Dong et al. 2022a); Heigouliang and Dongheigou in the eastern Tian Shan (Xue et al. 2013; Wang et al. 2016); Tuwaxincun (Tuva New Village) in the Altai (Dong et al. 2022b); Saragash, Grishkin, Urilkov Ulus, and Okunev Ulus in the Minusinsk Basin (Svyatko et al. 2021); Frinkent and Tashbulak near the southern Tian Shan (Hermes et al. 2018); as well as the Wulasitai and Xiaxingguang sites examined in this study (Figure 6).

An examination of the geographic distribution of mean $\delta^{13}C$ values for each site (Figure 6) reveals that within every regional subzone—including central Kazakhstan, the Minusinsk Basin, the Altai, the central Tian Shan, and the eastern Tian Shan—populations adhering to predominantly C_3-based diets coexisted spatially with groups consuming mixed C_3/C_4 diets. This pattern clearly cannot be explained solely by the dispersal or availability of millet. Instead, it points to differential subsistence choices within the same ecological and cultural landscapes.

Such variability suggests that the adoption of C_4 crops was neither inevitable nor uniform but rather mediated by a combination of local environmental constraints, economic strategies, mobility patterns, and cultural preferences. Understanding why certain communities or households maintained predominantly C_3-based diets while others incorporated C_4 crops requires moving beyond diffusionist models of crop spread and instead considering how agro-pastoral populations actively negotiated subsistence options in response to landscape, climate, and social context.

The reasons underlying this variability are complex. Ventresca-Miller et al. (2023) have argued that although millet can grow under semi-arid conditions, adequate water availability and fertile soils remain necessary for its successful cultivation and long-term incorporation into subsistence systems. In addition, temperature decline associated with increasing elevation, together with landscape aridification, constrained the adoption of C_4 crops in high-altitude environments (Wang et al. 2020a) . Beyond environmental factors, differences in individual- and community-level decision-making also played an important role in shaping subsistence strategies and dietary choices (Lightfoot et al. 2015).

To further evaluate these factors, this study compares the modern environmental settings of the sites discussed above. Relationships between mean $\delta^{13}C$ values and growing-season climatic variables provide important insights into how environmental constraints may have structured subsistence choices. Pearson's correlation coefficients and Spearman's rank correlations were calculated to assess associations between $\delta^{13}C$ values and two key variables: accumulated precipitation during the growing season (GSP) and the number of growing degree days above 10 °C (NGD10).

During the Early Iron Age, $\delta^{13}C$ values show a negative correlation with GSP. Linear regression models yield R^2 values ranging from 0.210 to 0.351, with Pearson's r values between −0.041 and −0.542 ($p = 2.27 \times 10^{-9}$ to 0.595) and Spearman's ρ values between −0.18 and −0.723 ($p = 2.27 \times 10^{-9}$ to 0.016). Higher $\delta^{13}C$ values—indicating a greater dietary contribution from millet (C_4 crops)—are more frequently associated with regions experiencing lower growing-season precipitation. This pattern suggests that communities in drier environments preferentially adopted millet, supporting earlier arguments that millet cultivation was favoured under arid conditions because of its drought tolerance (Jiang et al. 2013). It should be noted, however, that millet can also be cultivated in regions with higher precipitation; consequently, elevated $\delta^{13}C$ values in areas with high GSP are not anomalous and likely reflect broader agricultural flexibility.

In contrast, $\delta^{13}C$ values exhibit a moderate positive correlation with NGD10 during the Early Iron Age. Linear regression results show R^2 values between 0.235 and 0.351, Pearson's r values between 0.487 and 0.592 ($p = 1.73 \times 10^{-14}$ to 1.38×10^{-11}), and Spearman's ρ values between 0.493 and 0.592 ($p = 1.51 \times 10^{-6}$ to 6.35×10^{-2}). This pattern is consistent with previous findings that $\delta^{13}C$ values in the Tian Shan region increase with elevation during the Bronze Age and Early Iron Age (Wang et al. 2020a). Fundamentally, this relationship reflects temperature constraints associated with altitude: wheat and barley are more tolerant of low temperatures than millet (Anderson et al. 1995; Porter and Gawith 1999; Kamkar et al. 2006), making them more suitable for colder, high-altitude environments.

Fig. 7 further indicates that during the historical period (after AD 1), patterns of crop selection in the Tian Shan region changed. This may partly reflect smaller sample sizes for this period (n = 77) compared with the Early Iron Age (EIA-I: n = 171; EIA-II: n = 105; EIA-III: n = 172). However, it is also likely related to broader socio-economic transformations, including the intensification of interregional interaction following the development of the Silk Road. Increased mobility, trade, and food exchange during historical periods may have led to more homogenised C_3/C_4 dietary patterns. As shown in Figure 6d, $\delta^{13}C$ values along the Tian Shan during this period largely fall within the −18‰ to −15‰ range, indicating broadly mixed diets.

In addition, the construction of irrigation infrastructure—most notably *karez* (qanat) systems, which first appear in the historical period rather than prehistory (Bertrand 2010)—and other water-management facilities in Tian Shan valleys (Li et al. 2020; Kočár et al. 2026) would have expanded access to riverine water resources. Such developments reduced reliance on local precipitation and further weakened the direct coupling between climate variability and crop choice.

Together, these results demonstrate that long-term subsistence strategies in the Tian Shan were shaped by an interplay of environmental constraints, technological innovations, and social connectivity, rather than by crop availability alone.

As recorded by Ellsworth Huntington in his 1907 travel account *The Pulse of Asia*, local inhabitants of Xinjiang told him that:

"Indian corn, one of the great staples of Xinjiang*, will not grow at all. It is replaced by a large-grained variety of white millet. Wheat fares better, but only the first year. It a given field is cultivated two or three years in succession, it becomes worthless. Evidently, the permanent occupation of the lower Tarim and Konche regions by a fixed agricultural population is, under present conditions of irrigation, impossible even at Kara-Kum, the site farthest upstream. At Lulan, over two hundred miles farther downstream, where evaporation has had still more opportunity to concentrate the salt in the river, conditions must be much worse." (Huntington 1907, p. 268).

Water availability and limited irrigation capacity have long been key constraints on the cultivation of wheat and barley. Variability in precipitation, access to water resources, and the possible emergence of irrigation practices during the Early Iron Age (Li et al. 2017) would all have influenced patterns of crop production. Consequently, future research into ancient crop selection and subsistence strategies in the Tian Shan should adopt a multi-scalar approach that integrates palaeoenvironmental change, including temperature and precipitation variability, with archaeological evidence for water management and agricultural practice.

* The designation *Chinese Turkestan*, employed by Western explorers during the late Qing dynasty, carries strong colonial overtones; it is therefore replaced here with the term *Xinjiang*.

5. Conclusion

This study provides the first long-term, high-resolution carbon and nitrogen stable isotope dataset for the Wulasitai Valley, offering new insights into subsistence strategies in the Middle Tian Shan from the Early Iron Age to the late historical period (900 BC–AD 1400). The relative stability of $\delta^{15}N$ values through time indicates sustained access to animal-derived protein, including meat and dairy products. A small number of individuals, however, exhibit very low $\delta^{15}N$ values, likely reflecting episodes of resource stress or limited access to animal protein rather than long-term dietary norms.

In contrast, temporal fluctuations in $\delta^{13}C$ values reveal variable incorporation of C_4 plants, particularly millet. These shifts were neither linear nor uniform and do not indicate a permanent transition to C_4-based subsistence. Instead, periods of increased millet consumption—most notably around ca. 300–100 BC—correlate closely with episodes of environmental instability documented in regional palaeoclimate records. This pattern suggests that dietary flexibility functioned as a risk-management strategy, enabling communities to buffer climatic stress and fluctuating resource availability.

At a broader spatial scale, Early Iron Age populations in the Tian Shan did not display marked geographic heterogeneity in C_3/C_4 consumption. As demonstrated in this study, such variability is closely linked to growing-season precipitation and temperature, underscoring the importance of local ecological constraints—particularly thermal conditions and water availability—in shaping crop choice. These findings highlight the decisive role of microclimatic variation in mediating the adoption and persistence of different agricultural strategies.

More broadly, this research contributes to a growing body of evidence challenging homogenised models of Eurasian pastoralism. By situating the Wulasitai Valley within the wider Tian Shan and Central Asian context, this study highlights the diversity, resilience, and long-term adaptability of mountain agro-pastoral communities. The results emphasise the need to

rethink subsistence systems in the Tian Shan not as static or marginal, but as dynamic strategies shaped by complex interactions among environment, mobility, and cultural choice.

Declarations

Acknowledgements

This research was supported by the Major Special Project of the Ministry of Education's Philosophical and Social Sciences Research (2024), A Comparative Study on the Origins of Chinese and Foreign Civilisations (2024JZDZ058); the Archaeological Talent Promotion Programme of China (2024-267); and the Opening Foundation of the China–Central Asia "Belt and Road" Joint Laboratory on Human–Environment Research.

The authors would like to express their sincere gratitude to Professor Xiaozhong Huang and Dr. Liqiong Xiang (College of Earth and Environmental Sciences, Lanzhou University) for generously providing access to published sedimentary data from Bosten Lake.

Contributions

Ying Zhang and Kangte He wrote the main manuscript and contributed equally to this work. Ying Zhang prepared Figures 1–4, while Kangte He prepared Figures 5 and 6. Xiangpeng Zhang and Xiang Liu jointly conducted the excavation of the Wulasitai Valley sites and collected the samples. Xiang Liu supervised the study and the preparation of the manuscript. All authors reviewed and approved the final manuscript.

References

1. Ambrose SH, DeNiro MJ (1986) Reconstruction of African human diet using bone collagen carbon and nitrogen isotope ratios. Nature 319:321–324. https://doi.org/10.1038/319321a0
2. An C-B, Dong W, Li H, et al (2013) Correspondence regarding "Origin and spread of wheat in China" by Dodson, J.R., Li, X., Zhou, X., Zhao, K., Sun, N., Atahan, P. (2013), Quaternary Science Reviews 72, 108–111. Quaternary Science Reviews 81:148–149. https://doi.org/10.1016/j.quascirev.2013.09.010
3. Ananyevskaya E, Aytqaly AK, Beisenov AZ, et al (2018) Early indicators to C4 plant consumption in central Kazakhstan during the Final Bronze Age and Early Iron Age based on stable isotope analysis of human and animal bone collagen. Archaeological Research in Asia 15:157–173. https://doi.org/10.1016/j.ara.2017.12.002
4. Anderson P, Oelke E, Simmons S (1995) Growth and development guide for spring barley
5. Ban G (1962) Xiyu zhuan (Treatise on the Western Regions), juan 96, part 1 (shang). In: Hanshu. Zhonghua Shuju, Beijing, p 3921
6. Barton L, Newsome SD, Chen F-H, et al (2009) Agricultural origins and the isotopic identity of domestication in northern China. Proceedings of the National Academy of Sciences 106:5523–5528. https://doi.org/10.1073/pnas.0809960106
7. Bellér-Hann I (2008) Community matters in Xinjiang, 1880-1949: towards a historical anthropology of the Uyghur. Brill
8. Bertrand A (2010) The hydraulic systems in Turfan (Xinjiang). The silk road 8:27–41
9. Betts A, Jia PW, Dodson J (2014) The origins of wheat in China and potential pathways for its introduction: A review. Quaternary International 348:158–168. https://doi.org/10.1016/j.quaint.2013.07.044
10. Bleasdale M, Wotzka H-P, Eichhorn B, et al (2020) Isotopic and microbotanical insights into Iron Age agricultural reliance in the Central African rainforest. Commun Biol 3:619. https://doi.org/10.1038/s42003-020-01324-2
11. Bocherens H, Drucker D (2003) Trophic level isotopic enrichment of carbon and nitrogen in bone collagen: case studies from recent and ancient terrestrial ecosystems. International Journal of osteoarchaeology 13:46–53. https://doi.org/10.1002/oa.662

12. Brun P, Zimmermann NE, Hari C, et al (2022a) CHELSA-BIOCLIM+ A novel set of global climate-related predictors at kilometre-resolution
13. Brun P, Zimmermann NE, Hari C, et al (2022b) Global climate-related predictors at kilometer resolution for the past and future. Earth System Science Data 14:5573–5603
14. Cao H, Wang Z, He J, et al (2023) Performance and inter-comparison tests of the MICADAS at the radiocarbon laboratory of Lanzhou University, China. Radiocarbon 65:41–50
15. Chen F, Huang X, Zhang J, et al (2006) Humid Little Ice Age in arid central Asia documented by Bosten Lake, Xinjiang, China. SCI CHINA SER D 49:1280–1290. https://doi.org/10.1007/s11430-006-2027-4
16. Chen H-Y, Chen Y-J, Baker M (2012) Isotopic geochemistry of the Sawayaerdun orogenic-type gold deposit, Tianshan, northwest China: Implications for ore genesis and mineral exploration. Chemical Geology 310:1–11
17. Chen S (1964) Wendi ji (Annals of Emperor Wen), Wei shu 2, juan 2. In: Pei S (ed) Sanguozhi. Zhonghua Shuju, Beijing
18. Chen X, Guo X, Wang W, et al (2017a) The subsistence patterns of the Shengedaliang site (~4,000 yr BP) revealed by stable carbon and nitrogen isotopes in northern Shaanxi, China. Sci China Earth Sci 60:268–276. https://doi.org/10.1007/s11430-016-5123-8
19. Chen X, Yu J, You Y (2017b) Horse burial customs in Kalasu cemetery of Xinjiang seen from stable carbon and nitrogen isotope. W Reg Stud 4:89–98
20. Coplen TB (2011) Guidelines and recommended terms for expression of stable-isotope-ratio and gas-ratio measurement results. Rapid Communications in Mass Spectrometry 25:2538–2560. https://doi.org/10.1002/rcm.5129
21. Cosmo ND (1996) Ancient Xinjiang Between Central Asia and China; The Nomadic Factor. Anthropology & Archeology of Eurasia 34:87–101. https://doi.org/10.2753/AAE1061-1959340487
22. Dai Q, Wang A, Wang L, et al (2025) Diet of ancient Turban population from northwestern China illustrated by isotopic analysis of human teeth and bones. npj Herit Sci 13:142. https://doi.org/10.1038/s40494-025-01696-w
23. D'Alpoim Guedes J, Butler EE (2014) Modeling constraints on the spread of agriculture to Southwest China with thermal niche models. Quaternary International 349:29–41. https://doi.org/10.1016/j.quaint.2014.08.003
24. Deocampo DM (2010) The geochemistry of continental carbonates. Developments in Sedimentology 62:1–59. https://doi.org/10.1016/S0070-4571(09)06201-3
25. Dodson JR, Li X, Zhou X, et al (2013) Origin and spread of wheat in China. Quaternary Science Reviews 72:108–111. https://doi.org/10.1016/j.quascirev.2013.04.021
26. Dong W (2021) Diet of prehistoric residents of the Hami Basin. Fudan University Press, Shanghai
27. Dong W, An C, Zhang T, Alipujiang N (2022a) Subsistence strategies of people from Chawuhu Culture in the middle of Tianshan Mountains: A case study of Mohuchahan site from Hejing County, Xinjiang. Quaternary Sciences 42:80–91
28. Dong W, An C-B, Wang Y, et al (2021) Bone collagen stable isotope analysis of a Bronze Age site of Liushugou and its implication for subsistence strategy in arid northwest China. The Holocene 31:194–202. https://doi.org/10.1177/0959683620970259
29. Dong WM, An CB, Yu JJ, Chen XL (2022b) The subsistence strategy of the residents in the Bronze–early Iron Age Altay region and its implications: evidence from bone stable isotopes. West Reg Stud 1:45–54
30. Editorial Committee of Encyclopedia of Rivers and Lakes in China (2014) Section of River Basins in Northwest Region. China Water & Power Press, Beijing
31. Endo E, Shoda S, Frachetti M, et al (2023) Pottery Impressions Reveal Earlier Westward Dispersal of Foxtail Millet in Inner Asian Mountain Corridor. Agronomy 13:1706. https://doi.org/10.3390/agronomy13071706
32. Fan Y (1965) Xiyu zhuan (Treatise on the Western Regions), juan 88. In: Li X, others (eds) Hou Hanshu. Zhonghua Shuju, Beijing, p 2909
33. Fang X (1974a) Xuandi (Annals of Emperor Xuan), Di ji 1, juan 1. In: Jinshu. Zhonghua Shuju, Beijing

34. Fang X (1974b) Wudi (Annals of Emperor Wu), Di ji 3, juan 3. In: Jinshu. Zhonghua Shuju, Beijing
35. Fang X (1974c) Siyi (Biographies of the Four Barbarians), liezhuan 67, juan 97. In: Jinshu. Zhonghua Shuju, Beijing
36. Fang X (1974d) Jinshu. Zhonghua Shuju, Beijing
37. Frachetti MD (2012) Multiregional emergence of mobile pastoralism and nonuniform institutional complexity across Eurasia. Current Anthropology 53:2–38
38. Frachetti MD, Spengler RN, Fritz GJ, Mar'yashev AN (2010) Earliest direct evidence for broomcorn millet and wheat in the central Eurasian steppe region. Antiquity 84:993–1010. https://doi.org/10.1017/S0003598X0006703X
39. Gao Z, He K, Liu X (2026) New Radiocarbon Dates and Modelling Reveal the Prehistoric Chronology and Multiple Interments in the Wulasitai Valley, Middle Tian Shan Region in Hejing County (Xinjiang Uygur Autonomous Region, China). Radiocarbon
40. Geng S, Zhang G (2008) Suolimi kao□□□□□□□ / A Study of Suolimi□. In: Zhang G (ed) Wenshu, Dianji yu Xiyu Shi-Di□□□□□□□ □□□□□□ / Documents, Texts, and the Historical Geography of the Western Regions□. Guangxi Normal University Press, Guilin
41. Gierlowski-Kordesch EH (2010) Lacustrine carbonates. Developments in sedimentology 61:1–101. https://doi.org/10.1016/S0070-4571(09)06101-9
42. Graham NE, Ammann CM, Fleitmann D, et al (2011) Support for global climate reorganization during the "Medieval Climate Anomaly." Clim Dyn 37:1217–1245. https://doi.org/10.1007/s00382-010-0914-z
43. Guo Y, Lou J, Xie S, et al (2020) Isotopic reconstruction of human diet in the Ji'erzankale site, Xinjiang Uyghur Autonomous Region, China. International Journal of Osteoarchaeology 30:65–72. https://doi.org/10.1002/oa.2831
44. Hedges REM, Reynard LM (2007) Nitrogen isotopes and the trophic level of humans in archaeology. Journal of Archaeological Science 34:1240–1251. https://doi.org/10.1016/j.jas.2006.10.015
45. Hermes TR, Frachetti MD, Bullion EA, et al (2018) Urban and nomadic isotopic niches reveal dietary connectivities along Central Asia's Silk Roads. Scientific Reports 8:5177
46. Hermes TR, Frachetti MD, Doumani Dupuy PN, et al (2019) Early integration of pastoralism and millet cultivation in Bronze Age Eurasia. Proceedings of the Royal Society B 286:20191273
47. Hong Y (ed) (1995) Hejing Xianzhi [Hejing County Annals]. Xinjiang People's Publishing House, Urumqi
48. Hu Y, He D, Dong Y, et al (2006) Shandong Tengzhou Xigongqiao yizhi rengu de wending tongweisu fenxi (Stable isotopic analysis on human remains from Xigongqiao, Tengzhou, Shandong). Disiji Yanjiu (Quaternay Sciences) 25:561–7
49. Huang W (1989) Han tong Xiyu hou dui Xiyu zhi yingxiang (The Impact of Han Contacts with the Western Regions on the Western Regions). In: Huang L (ed) Huang Wenbi lishi kaogu lunji. Wenwu Chubanshe, Beijing
50. Huang X, Huang C, Xu Y, et al (2023) Body size of fossil *Pediastrum* in lake sediments as an indicator of temperature variation. Palaeogeography, Palaeoclimatology, Palaeoecology 625:111687. https://doi.org/10.1016/j.palaeo.2023.111687
51. Huang X, Xiang L, Lei G, et al (2021) Sedimentary *Pediastrum* record of middle–late Holocene temperature change and its impacts on early human culture in the desert-oasis area of northwestern China. Quaternary Science Reviews 265:107054. https://doi.org/10.1016/j.quascirev.2021.107054
52. Huang X, Zhou G, Ma Y, et al (2010) Pollen distribution in large freshwater lake of arid region: a case study on the surface sediments from Bosten Lake, Xinjiang, China. Front Earth Sci China 4:174–180. https://doi.org/10.1007/s11707-009-0060-2
53. Huang XZ, Chen FH, Fan YX, Yang ML (2009) Dry late-glacial and early Holocene climate in arid central Asia indicated by lithological and palynological evidence from Bosten Lake, China. Quaternary International 194:19–27. https://doi.org/10.1016/j.quaint.2007.10.002

54. Huntington E (1907) The Pulse of Asia: A Journey in Central Asia Illustrating the Geographic Basis of History. Houghton, Mifflin
55. Ivanovich SP, Petrovich SD (2020) The cultures of the Early Iron Age in China as part of the Scythian world. Materialy po arkheologii i istorii antichnogo i srednevekovogo Prichernomor'ya 12:111–147
56. Kamkar B, Koocheki A, Mahallati MN, Moghaddam PR (2006) Cardinal temperatures for germination in three millet species (Panicum miliaceum, Pennisetum glaucum and Setaria italica).
57. Kočár P, Sůvová Z, Vatansever A, et al (2026) A water reservoir from the 3rd to 5th century AD as a possible key for understanding the subsistence strategies and environment at the margin of the Fergana basin in Southern Kyrgyzstan. Archaeological and Anthropological Sciences 18:37
58. Kuropatkin AN (1882) Kasiigaria: Historical and Geographical Sketch of the Country; Its Military Strength, Industries and Trade. Calcutta
59. Lee-Thorp JA (2008) On Isotopes and Old Bones*. Archaeometry 50:925–950. https://doi.org/10.1111/j.1475-4754.2008.00441.x
60. Leng MJ, Marshall JD (2004) Palaeoclimate interpretation of stable isotope data from lake sediment archives. Quaternary Science Reviews 23:811–831. https://doi.org/10.1016/j.quascirev.2003.06.012
61. Li H, Wang B, Yang X, et al (2025) Ancient genomes shed light on the genetic history of the Iron Age to historical central Xinjiang, northwest China. BMC Biol 23:93. https://doi.org/10.1186/s12915-025-02195-x
62. Li Y (1974) Xiyu (Western Regions), juan 97. In: Beishi. Zhonghua Shuju, Beijing, p 3212
63. Li Y (2021) Agriculture and palaeoeconomy in prehistoric Xinjiang, China (3000–200 bc). Veget Hist Archaeobot 30:287–303. https://doi.org/10.1007/s00334-020-00774-2
64. Li Y, Storozum MJ, Jia X, et al (2020) Reconceptualizing water history of Chinese Central Asia: Hydraulic modeling of the early 1st mill. AD irrigation system at Mohuchahangoukou-4 (MGK4), Xinjiang, China. Journal of Archaeological Science: Reports 33:102534. https://doi.org/10.1016/j.jasrep.2020.102534
65. Li Y, Storozum MJ, Wang X, Guo W (2017) Early irrigation and agropastoralism at Mohuchahangoukou (MGK), Xinjiang, China. Archaeological Research in Asia 12:23–32. https://doi.org/10.1016/j.ara.2017.09.005
66. Li Z (ed) (2012) Xiyu shidi san zhong ziliao jiaozhu□□□□□□□□□□□□□□ / Collated and Annotated Materials on the Historical Geography of the Western Regions□. Xinjiang Renmin Chubanshe, Urumqi
67. Lightfoot E, Motuzaite-Matuzeviciute G, O'Connell TC, et al (2015) How 'Pastoral' is Pastoralism? Dietary Diversity in Bronze Age Communities in the Central Kazakhstan Steppes. Archaeometry 57:232–249. https://doi.org/10.1111/arcm.12123
68. Liu B, Turuhan B, Keremu A, Liu X (2018) Vertical distribution patterns of the seed plant flora in the middle section on the southern slopes of the Tianshan Mountains in Xinjiang, China.
69. Liu X (1975) Dili zhi (Geographical Treatise), juan 40, part 3. In: Jiutangshu. Zhonghua Shuju, Beijing
70. Liu Y (2006) Chaha tai Hanguo shi yanjiu□□□□□□□□□□□□ / A Study of the History of the Chaghatai Khanate□. Shanghai Guji Chubanshe, Shanghai
71. Long T, Leipe C, Jin G, et al (2018) The early history of wheat in China from 14C dating and Bayesian chronological modelling. Nature Plants 4:272–279. https://doi.org/10.1038/s41477-018-0141-x
72. Ma M, Dong G, Jia X, et al (2016) Dietary shift after 3600 cal yr BP and its influencing factors in northwestern China: Evidence from stable isotopes. Quaternary Science Reviews 145:57–70
73. Mann ME, Zhang Z, Rutherford S, et al (2009) Global Signatures and Dynamical Origins of the Little Ice Age and Medieval Climate Anomaly. Science 326:1256–1260. https://doi.org/10.1126/science.1177303
74. Matuzeviciute GM, Ananyevskaya E, Sakalauskaite J, et al (2022) The integration of millet into the diet of Central Asian populations in the third millennium BC. Antiquity 96:560–574. https://doi.org/10.15184/aqy.2022.23

75. McCutchan Jr JH, Lewis Jr WM, Kendall C, McGrath CC (2003) Variation in trophic shift for stable isotope ratios of carbon, nitrogen, and sulfur. Oikos 102:378–390. https://doi.org/10.1034/j.1600-0706.2003.12098.x
76. Mekonnen MM, Hoekstra AY (2011) The green, blue and grey water footprint of crops and derived crop products. Hydrology and Earth System Sciences 15:1577–1600. https://doi.org/10.5194/hess-15-1577-2011
77. Mingzhe W, Enguo L (1999) Xinjiang Chawuhu: Daxing shizu mudi fajue baogao (Chawuhu, Xinjiang: Excavation Report of Large-scale Clan Cemetery)
78. Motuzaite Matuzeviciute G, Lightfoot E, O'Connell TC, et al (2015) The extent of cereal cultivation among the Bronze Age to Turkic period societies of Kazakhstan determined using stable isotope analysis of bone collagen. Journal of Archaeological Science 59:23–34. https://doi.org/10.1016/j.jas.2015.03.029
79. Murphy EM, Schulting R, Beer N, et al (2013) Iron Age pastoral nomadism and agriculture in the eastern Eurasian steppe: implications from dental palaeopathology and stable carbon and nitrogen isotopes. Journal of Archaeological Science 40:2547–2560. https://doi.org/10.1016/j.jas.2012.09.038
80. Narasimhan VM, Patterson N, Moorjani P, et al (2018) The genomic formation of South and Central Asia. Biorxiv 292581
81. O'Connell TC, Kneale CJ, Tasevska N, Kuhnle GGC (2012) The diet-body offset in human nitrogen isotopic values: a controlled dietary study. Am J Phys Anthropol 149:426–434. https://doi.org/10.1002/ajpa.22140
82. Oleszczak L, Pokutta D, Chugunov K, Götherström A (2023) The food culture of the Iron Age nomadic elite from the 'Valley of the Kings' in Tuva: radiocarbon dating, stable carbon and nitrogen analysis of the Chinge Tey barrows (Turan-Uyuk Basin, Russia). Journal of Archaeological Science: Reports 51:104186. https://doi.org/10.1016/j.jasrep.2023.104186
83. Ouyang X, Song Q (1975) Xiyu liezhuan (Biographies of the Western Regions), juan 221, part 1. In: Xintangshu. Zhonghua Shuju, Beijing, p 6228
84. Pechenkina EA, Ambrose SH, Xiaolin M, Benfer RA (2005) Reconstructing northern Chinese Neolithic subsistence practices by isotopic analysis. Journal of Archaeological Science 32:1176–1189. https://doi.org/10.1016/j.jas.2005.02.015
85. Porter JR, Gawith M (1999) Temperatures and the growth and development of wheat: a review. European journal of agronomy 10:23–36
86. Ramsey CB (2009) Bayesian analysis of radiocarbon dates. Radiocarbon 51:337–360
87. Ramsey CB (2021) OxCal 4.4. 4 calibration program. Website: https://c14 arch ox ac uk/oxcal/OxCal html
88. Reimer PJ, Austin WE, Bard E, et al (2020) The IntCal20 Northern Hemisphere radiocarbon age calibration curve (0–55 cal kBP). Radiocarbon 62:725–757
89. Riccomi G, Minozzi S, Zech J, et al (2020) Stable isotopic reconstruction of dietary changes across Late Antiquity and the Middle Ages in Tuscany. Journal of Archaeological Science: Reports 33:102546. https://doi.org/10.1016/j.jasrep.2020.102546
90. Schoeninger MJ, DeNiro MJ, Tauber H (1983) Stable Nitrogen Isotope Ratios of Bone Collagen Reflect Marine and Terrestrial Components of Prehistoric Human Diet. Science 220:1381–1383. https://doi.org/10.1126/science.6344217
91. Shulga PI, Shulga DP, Hasnulina KA (2019) Mohuchahan: Early Scythian Age Burial Ground in Xinjiang. Vestnik NSU Series: History and Philology 18:19–29
92. Si Y, Lu E, Li X, et al (2013) Xinjiang Yanghai mudi xianmin de shiwu jiegou ji renqun zucheng tansuo (□□□□□□□□□□□□□□□□□□□□□□□□□□ / Dietary Structure and Population Composition of the Ancient Inhabitants of the Yanghai Cemetery, Xinjiang). Kexue tongbao (□□□□ / Chinese Science Bulletin) 58:1422–1429
93. Strauss A, Oliveira RE, Villagran XS, et al (2016) Early Holocene ritual complexity in South America: thearchaeological record of Lapa do Santo (east-central Brazil). Antiquity 90:1454–1473. https://doi.org/10.15184/aqy.2016.220
94. Sun S (2024) Study of the Periodization and Chronology of the Chawuhu Culture. Archaeological Collectanea 101–122

95. Svyatko SV, Schulting RJ, Papin D, Reimer PJ (2021) MILLET CONSUMPTION IN SIBERIA PRIOR TO MID-SECOND MILLENNIUM BC? A REVIEW OF RECENT DEVELOPMENTS. Radiocarbon 63:1547–1554. https://doi.org/10.1017/RDC.2021.53
96. Talbot MR (1990) A review of the palaeohydrological interpretation of carbon and oxygen isotopic ratios in primary lacustrine carbonates. Chemical Geology: Isotope Geoscience section 80:261–279. https://doi.org/10.1016/0168-9622(90)90009-2
97. Tian D, Festa M, Cong D, et al (2021) New evidence for supplementary crop production, foddering and fuel use by Bronze Age transhumant pastoralists in the Tianshan Mountains. Sci Rep 11:13718. https://doi.org/10.1038/s41598-021-93090-2
98. Ventresca-Miller AR, Wilkin S, Smithers R, et al (2023) Adaptability of Millets and Landscapes: Ancient Cultivation in North-Central Asia. Agronomy 13:. https://doi.org/10.3390/agronomy13112848
99. Wang L, Zhang G, Wang Y, et al (2024) Prehistoric subsistence strategy dynamics and their differences under a similar hyper-arid environment in the contiguous Turpan and Hami Basins of Xinjiang. The Holocene 34:1154–1163. https://doi.org/10.1177/09596836241247306
100. Wang T, Wei D, Chang X, et al (2019) Tianshanbeilu and the Isotopic Millet Road: reviewing the late Neolithic/Bronze Age radiation of human millet consumption from north China to Europe. National Science Review 6:1024–1039
101. Wang TT, Fuller BT, Wei D, et al (2016) Investigating Dietary Patterns with Stable Isotope Ratios of Collagen and Starch Grain Analysis of Dental Calculus at the Iron Age Cemetery Site of Heigouliang, Xinjiang, China. International Journal of Osteoarchaeology 26:693–704. https://doi.org/10.1002/oa.2467
102. Wang W, Duan F, Zhang J, et al (2023) Gender differences in millet consumption in arid Inner Asia during the Iron Age documented by stable isotopes: A case study from Shihuyao, Xinjiang. Quaternary Science Reviews 312:108187. https://doi.org/10.1016/j.quascirev.2023.108187
103. Wang W, Liu Y, Duan F, et al (2020a) A comprehensive investigation of Bronze Age human dietary strategies from different altitudinal environments in the Inner Asian Mountain Corridor. Journal of Archaeological Science 121:105201. https://doi.org/10.1016/j.jas.2020.105201
104. Wang W, Liu Y, Duan F, et al (2020b) A comprehensive investigation of Bronze Age human dietary strategies from different altitudinal environments in the Inner Asian Mountain Corridor. Journal of Archaeological Science 121:105201
105. Wang X (1991) Lun Anxi sizhen Yanqi yu Suiye de jiaoti□□□□□□□□□□□□□□□□□ / On the Alternation of Yanqi and Suiye among the Four Anxi Garrisons□. Beijing Daxue Xuebao (Zhexue Shehui Kexue Ban)
106. Wang Y, Wang W, Liu L, et al (2020c) Reliability of the Artemisia/Chenopodiaceae pollen ratio in differentiating vegetation and reflecting moisture in arid and semi-arid China. The Holocene 30:858–864. https://doi.org/10.1177/0959683620902219
107. Wei S (1974) Xiyu liezhuan (Biographies of the Western Regions), juan 102. In: Weishu. Zhonghua Shuju, Beijing, p 2265
108. Wilkin S, Ventresca Miller A, Miller BK, et al (2020) Economic Diversification Supported the Growth of Mongolia's Nomadic Empires. Sci Rep 10:3916. https://doi.org/10.1038/s41598-020-60194-0
109. Wu G (2023) The Origin and Formation of the Archaeological Cultures in the Bronze Age Xinjiang. In: Wu G (ed) Archaeological Research on the Societies of Late Prehistoric Xinjiang, Vol 2. Springer Nature, Singapore, pp 61–141
110. Wu G (2022) Site Characteristics and Chronology of the Archaeological Remains in the Eastern Tianshan Mountain Region. In: Archaeological Research on the Societies of Late Prehistoric Xinjiang, Vol 1. Springer Nature Singapore, Singapore, pp 37–102
111. Wünnemann B, Mischke S, Chen F (2006) A Holocene sedimentary record from Bosten Lake, China. Palaeogeography, Palaeoclimatology, Palaeoecology 234:223–238. https://doi.org/10.1016/j.palaeo.2005.10.016

112. Xiang L, Chen X, Huang C, et al (2021) Divergent patterns of Holocene hydro-climatic evolution in arid central Asia and the Asian summer monsoon margin indicated by *Pediastrum* records. Palaeogeography, Palaeoclimatology, Palaeoecology 582:110662. https://doi.org/10.1016/j.palaeo.2021.110662
113. Xie C, Liu S, Cui Y, et al (2005) Analysis of mitochondrial DNA from the ancient tombs of Chawuhu. Journal of Jilin University (science Edition 43:538–540
114. Xie H, Liang J, Vachula RS, et al (2021) Changes in the hydrodynamic intensity of Bosten Lake and its impact on early human settlement in the northeastern Tarim Basin, Arid Central Asia. Palaeogeography, Palaeoclimatology, Palaeoecology 576:110499. https://doi.org/10.1016/j.palaeo.2021.110499
115. Xie M, Jiang H, Yang Y, others (2014) Xinjiang Keliya he beifang mudi chutuo shiwu yicun de zhiwu weitihua shi fenxi (/ Archaeobotanical Investigation of Ancient Cakes from the North Cemetery at the Keriya River, Xinjiang, Northwest China). Dongfang kaogu (/ East Asia Archaeology) 394–401
116. Xinjiang Uygur Autonomous Region Cultural Relics and Archaeology Institute (1999) Xinjiang chawuhu: daxing shizu mudi fajue baogao (The Chawuhu site in Xinjiang: Excavation report of a large clan cemetery). Oriental Press (Dongfang Chubanshe), Beijing
117. Xinjiang Uygur Autonomous Region Cultural Relics and Archaeology Institute (2016) The Mohuchahan Cemetery, Xinjiang (Xinjiang Mohuchahan Mudi). Science Press ( ), Beijing
118. Xu Q, Li Y, Yang X, Zheng Z (2007) Quantitative relationship between pollen and vegetation in northern China. SCI CHINA SER D 50:582–599. https://doi.org/10.1007/s11430-007-2044-y
119. Xue L, Xi C, Jian-xin W, et al (2013) Carbon and nitrogen isotopic analysis of human bones excavated from the Dongheigou site, Ba Li-kun County, Xinjiang Autonomous Region. Acta Anthropologica Sinica 32:219
120. Zhang Q, Chang X, Liu G (2009) Xinjiang Balikun xian Heigouliang mudi chutuo ren gu de shixing fenxi (/ Dietary Analysis of Human Remains from the Heigouliang Cemetery, Balikun County, Xinjiang). Xiyu yanjiu (/ The Western Regions Studies) 45–49
121. Zhang Q, Li S (2006) Xinjiang Nileke xian Qiongkeke yihao mudi gudai jumin de shiwu jiegou fenxi (/ Dietary Structure of Ancient Residents from the Qiongkeke No. 1 Cemetery in Nileke County, Xinjiang). Xiyu yanjiu (/ The Western Regions Studies) 78–81
122. Zhang X, Qiu S, Zhang J, Guo W (2014) Xinjiang Duogang mudi chutuo ren gu de tan-dan wending tongweisu fenxi (/ Stable Carbon and Nitrogen Isotope Analysis of Human Bones from the Duogang Cemetery, Xinjiang). Nanfang wenwu (/ Cultural Relics of Southern China) 79–91
123. Zheng M, Huang X, Wang N, et al (2025) Late Holocene extreme dust events in the arid Central Asia recorded by lake sediments in Tien Shan. Quaternary Science Reviews 368:109568. https://doi.org/10.1016/j.quascirev.2025.109568
124. Zhong W, Xiong H (1998) Isotopic evidence for holocene climatic changes in Bosten Lake, Southern Xinjiang, China. Chin GeographSc 8:176–182. https://doi.org/10.1007/s11769-997-0032-y
125. Zhou L, Garvie-Lok SJ (2015) Isotopic evidence for the expansion of wheat consumption in northern China. Archaeological Research in Asia 4:25–35. https://doi.org/10.1016/j.ara.2015.10.001
126. Zhou X, Yu J, Spengler RN, et al (2020) 5,200-year-old cereal grains from the eastern Altai Mountains redate the trans-Eurasian crop exchange. Nat Plants 6:78–87. https://doi.org/10.1038/s41477-019-0581-y

Figures

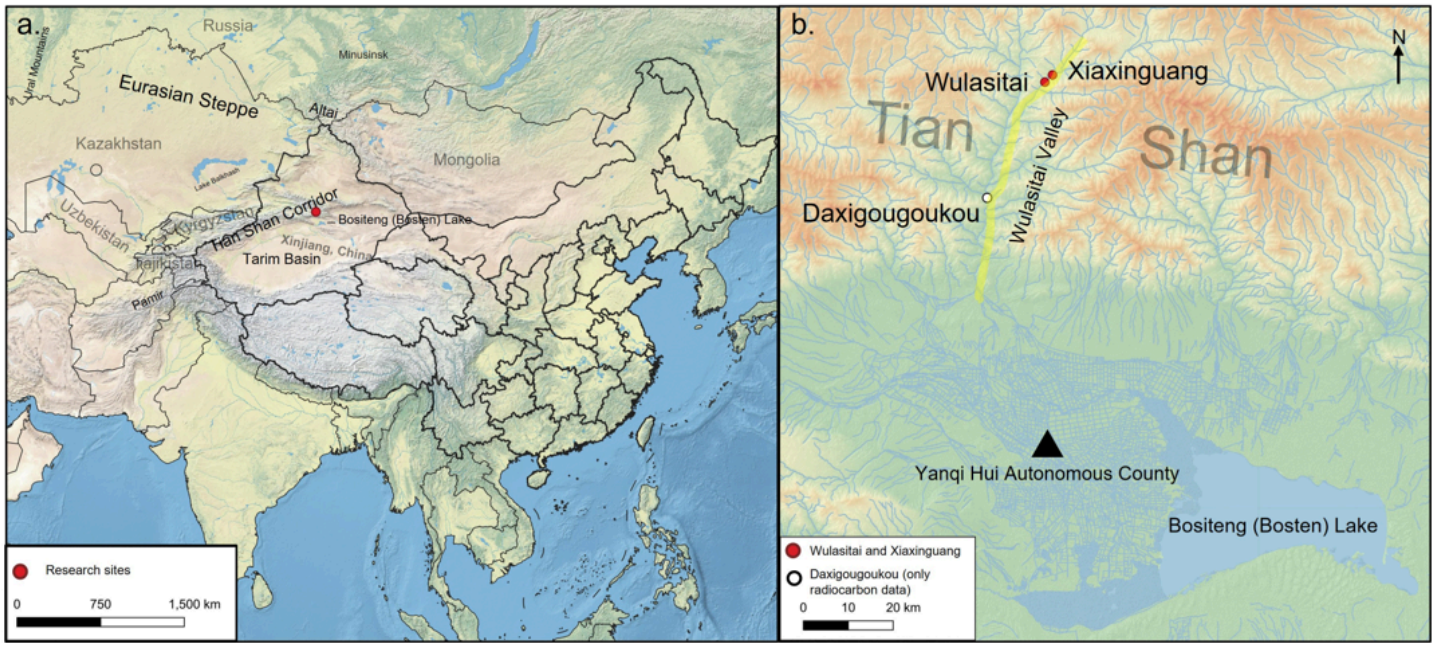


Figure 1

(a) Location of the research sites and their broader geographic context; (b) Detailed map of the study area showing the Wulasitai Valley (highlighted in yellow) and the locations of the investigated sites—Wulasitai and Xiaxingguang (both sampled for carbon and nitrogen stable isotope analysis and radiocarbon dating), and Daxigoukou (sampled for radiocarbon dating only). The valley lies close to Bositeng (Bosten) Lake, whose lacustrine sedimentary record provides high-resolution palaeoenvironmental data for the region. Maps were produced using QGIS. The base map derives from the Natural Earth 10m raster dataset, available at https://naciscdn.org/naturalearth/10m/raster/NE1_HR_LC_SR_W_DR.zip



Figure 2

Representative assemblages of artefacts from the Wulasitai Valley spanning the Early Iron Age (Early, Middle, and Late stages) and Historical Stages I–IV. From left to right: Early Iron Age (Early Stage): handled jar with spout, handled bowl, bronze and stone beads; Early Iron Age (Middle Stage): handled jar and handled pot, iron-handled bronze mirror; Early Iron Age (Late Stage): handled jar with markedly flared rim, painted handled pot, bronze pin, and horse bit; Historical Stage I: iron ring and stone object; Historical Stage II: jade ring and brass finger ring; Historical Stage III: silver cup, bronze mirror, painted wooden saddle, and gilt brocade; Historical Stage IV: bronze mirror and iron stirrup.

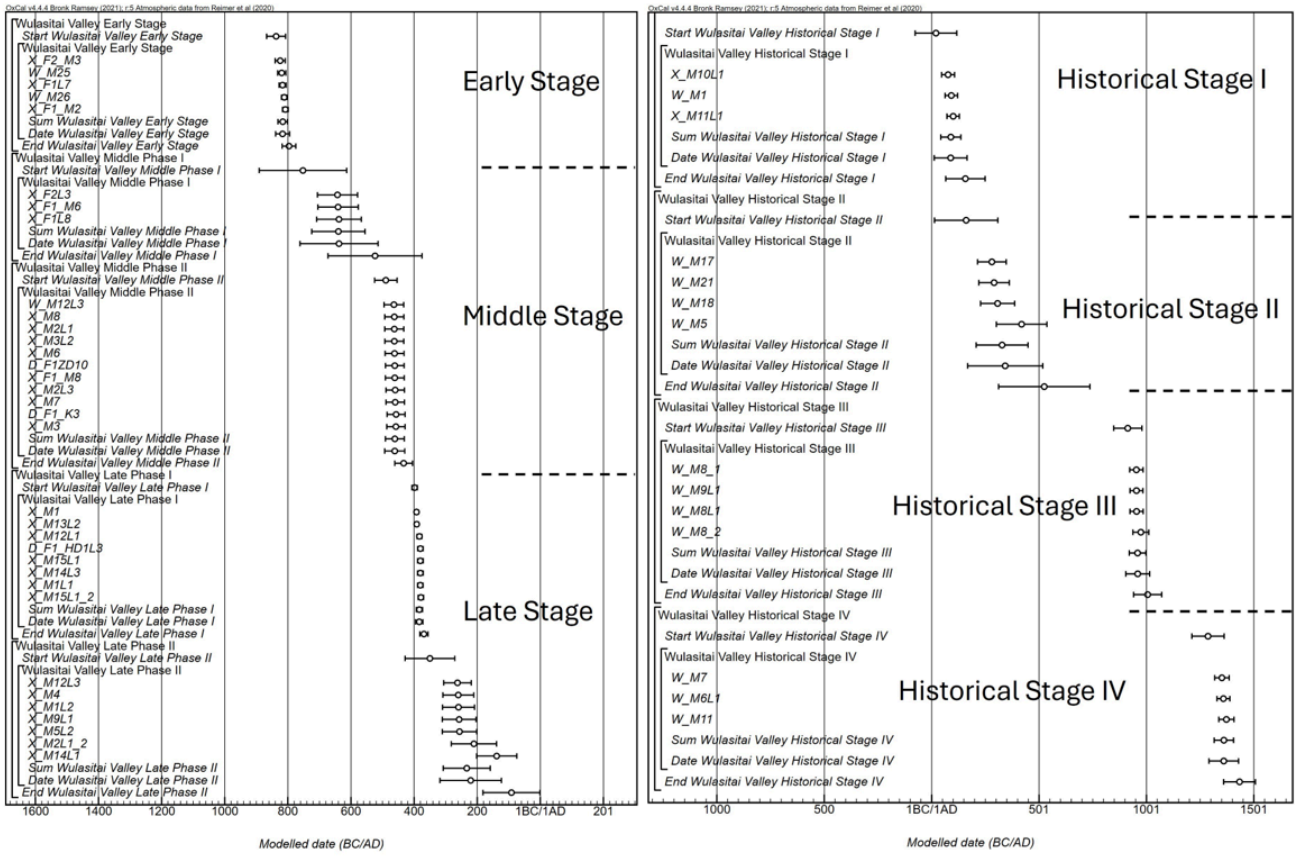


Figure 3

Radiocarbon dates from the Wulasitai Valley, illustrating the chronological sequence of the Early Iron Age (Early, Middle, and Late stages) and Historical Stages I–IV. Maps This figure is produced using Oxcal v.4.4, access to https://c14.arch.ox.ac.uk/oxcal/OxCal.html, the program can be found in supplementary materials

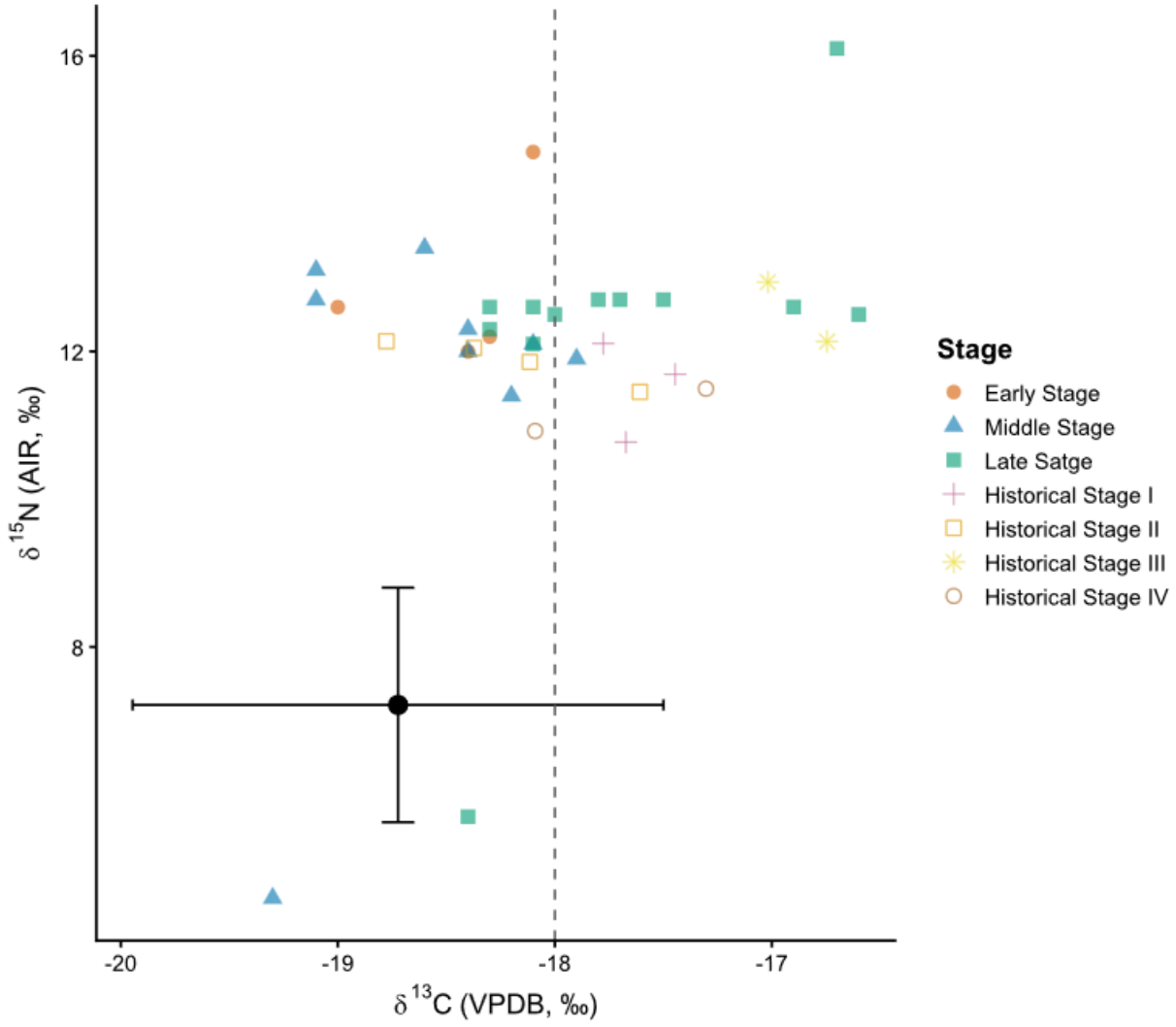


Figure 4

Showing the carbon and nitrogen isotopes data from Wulasitai valley in the different stages, the black error bar showing the CN isotopes data from herbivores in Xinjiang from Bronze Age to Historical stages (n = 234; mean = 7.21‰, data from Chen et al. 2017a; Guo et al. 2020; Dong 2021; Dong et al. 2021)

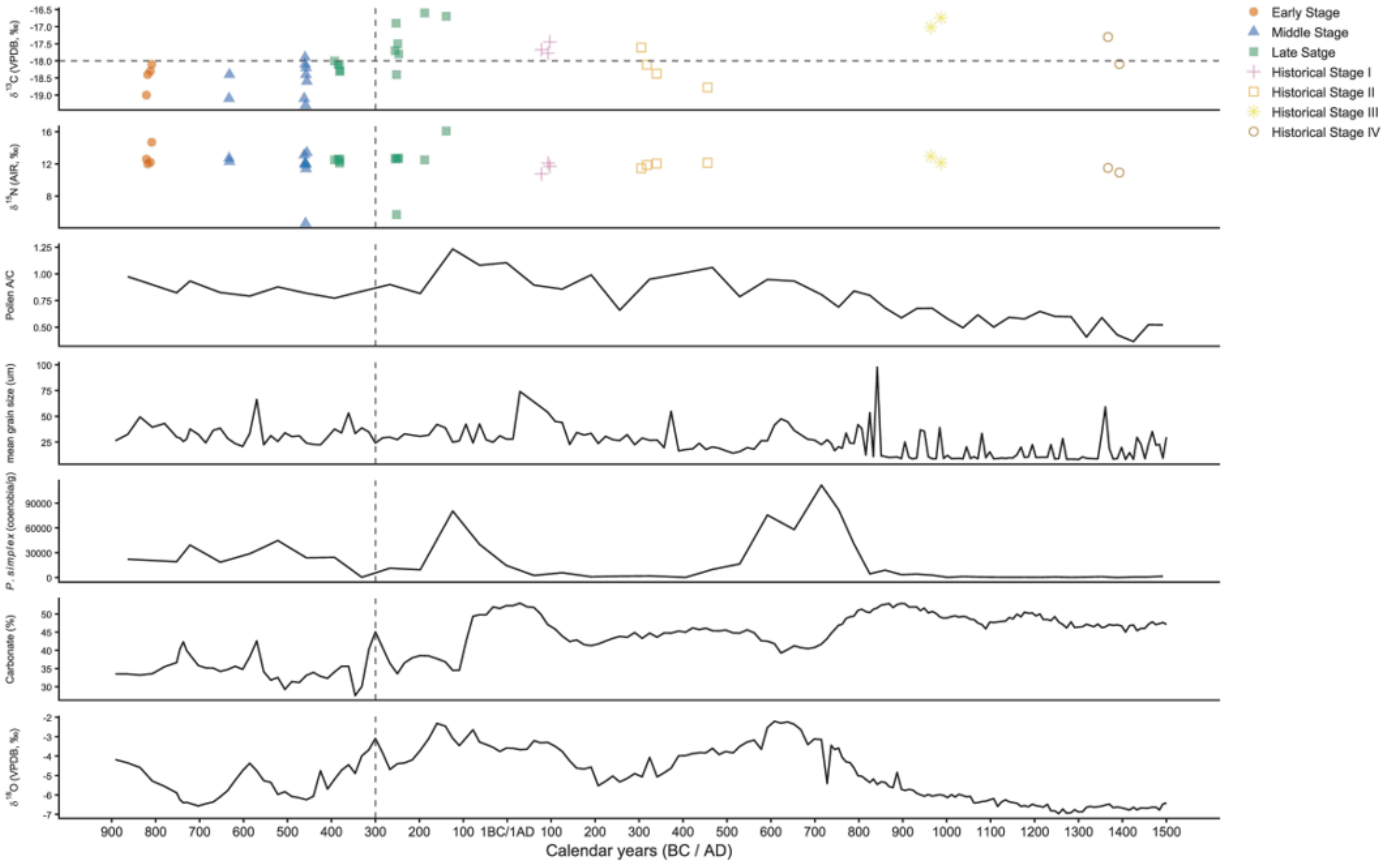


Figure 5

showing the change of δ¹³C (VPDB, ‰) and δ¹⁵N (AIR, ‰) values during calendar years in Wulasitai and environmental factors including Pollen A/C, mean grain size of sands (μm), and the *Pediastrum* concentrations (*p. simplex*, coenobia/g), carbonate concentrations (%) and δ¹⁸O (VPDB, ‰), data majorly from Huang et al. (2009, 2010, 2021).

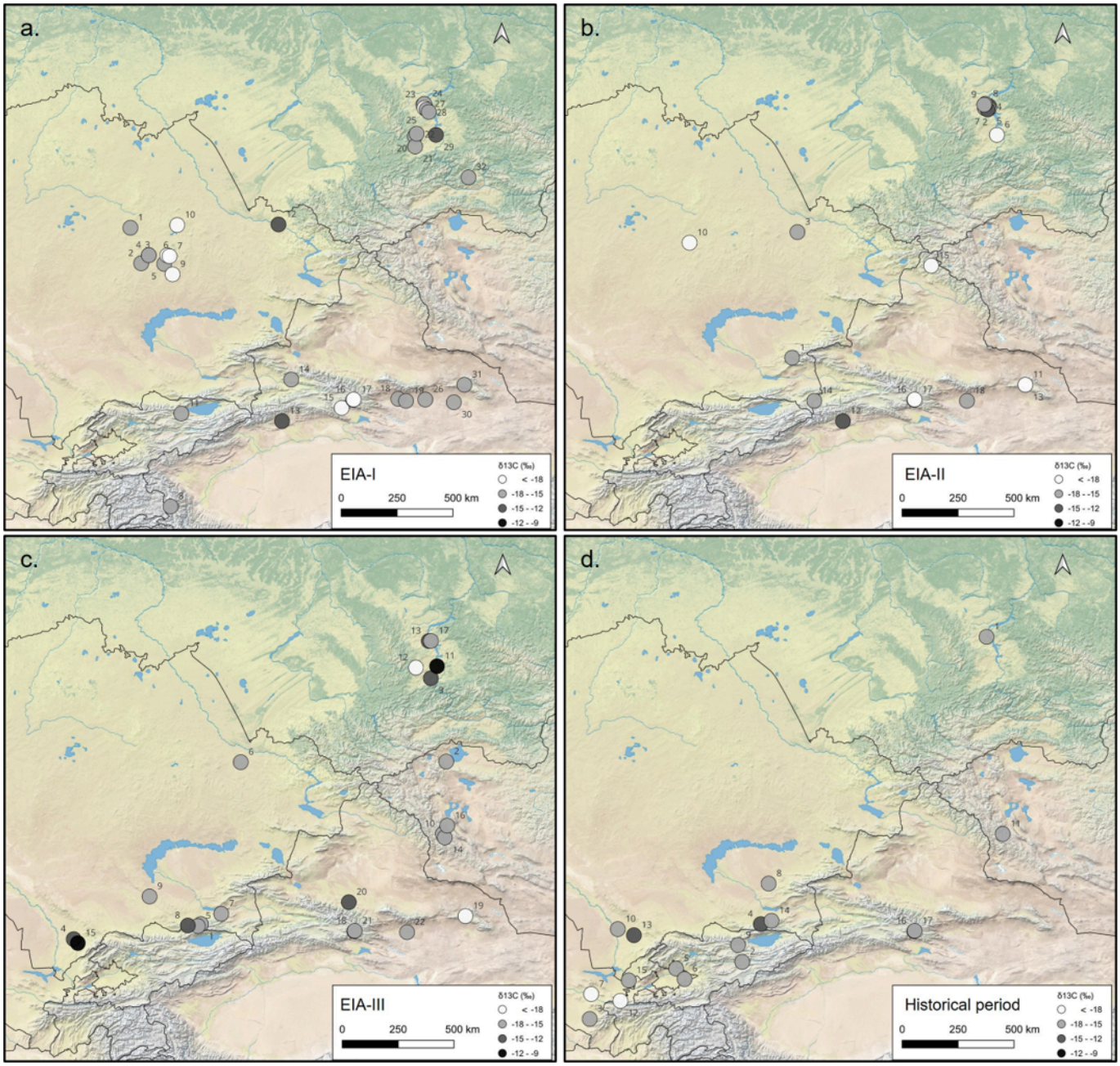


Figure 6

Mean $\delta^{13}C$ values (VPDB, ‰) of archaeological sites in the eastern Eurasian steppe and the Tian Shan region from Early Iron Age I (EIA-I) to the historical period (after AD 1). Colour shading indicates dietary composition: white (< −18‰) represents an almost exclusively C_3-based diet; light grey (−18 to −15‰), dark grey (−15 to −12‰), and black (−12 to −9‰) indicate increasing proportions of mixed C_3/C_4 diets, with darker shades reflecting a higher contribution of C_4 plants. (a) EIA-I (Early Iron Age I, 1000–700 BC): Tegiszhol; 2. Myrzhyk 6; 3. Akbeit; 4. Karashoky; 5. Karakemer; 6. Tandaily; 7. Baike 2; 8. Jierzankale; 9. Bakybulak; 10. Kyzylshilik; 11. Chap I; 12. Zevakinskiy; 13. Duogang; 14. Qiongkeke 1st Cemetery; 15. Mohuchahan; 16. Wulasitai; 17. Xiaxingguang; 18. Jiayi; 19. Yanghai; 20. Okunev Ulus; 21. Verhniy Askiz I; 22. Uibat V; 23. Saragash Ozero; 24. Saragash; 25. Grishkin Log 1; 26. Ya'er; 27. Podgornoye Ozero; 28. Yarki II; 29. Nurilkov Ulus; 30. Ailiekexia'er; 31. Dongheigou; 32. Chinge Tey I. (b) EIA-II (Early Iron Age II, 700–300 BC): Begash; 2. Karasuk III; 3. Kotyrkora; 4. Lepeshkina; 5. Melnichniy–Barsuchinniy Log; 6. Nurilkov Ulus; 7. Podgornoye Ozero; 8. Saragash; 9. Saragash Ozero; 10. Zhartas; 11. Dongheigou; 12. Duogang; 13. Heigouliang; 14. Kalasu; 15. Tuwaxincun; 16. Wulasitai; 17. Xiaxingguang; 18. Yanghai. (c) EIA-III (Early Iron Age III, 400 BC–AD 1: Alatau-1; 2. Chandman Mountain; 3. Chernoye Ozero I; 4. Kainarbulak-1;

5. Kamenka; 6. Karatobe; 7. Karatuma; 8. Kargaly-I; 9. Khatau-1; 10. Khoit Tsenkher (Tarvagatain Am); 11. Nurilkov Ulus; 12. Okunev Ulus; 13. Podgornoye Ozero; 14. Shombuuzyn-Belchir (SBR); 15. Shymkent; 16. Takhiltyn-Khotgor (THL); 17. Yarki I; 18. Wulasitai; 19. Dongheigou; 20. Shihuyao; 21. Xiaxingguang; 22. Yanghai. (d) Historical period (after AD 1): Afanasyeva Gora; 2. Aigyrzhal 1; 3. Altyntepe; 4. Butakty-1; 5. Chartok; 6. Chor Dona; 7. Frinkent; 8. Karatal; 9. Kok-Tash; 10. Konyr-Tebe-1; 11. Takhiltyn Khotgor; 12. Tashbulak; 13. Temirlanovka; 14. Turgen-2; 15. Uturlik Tepe; 16. Wulasitai; 17. Xiaxingguang (data from this study, Zhang and Li 2006; Zhang et al. 2009, 2014; Si et al. 2013; Xue et al. 2013; Lightfoot et al. 2015; Wang et al. 2016; Chen et al. 2017b; Narasimhan et al. 2018; Ananyevskaya et al. 2018; Hermes et al. 2019; Guo et al. 2020; Dong 2021; Svyatko et al. 2021; Dong et al. 2022a; Matuzeviciute et al. 2022; Oleszczak et al. 2023; Dai et al. 2025)

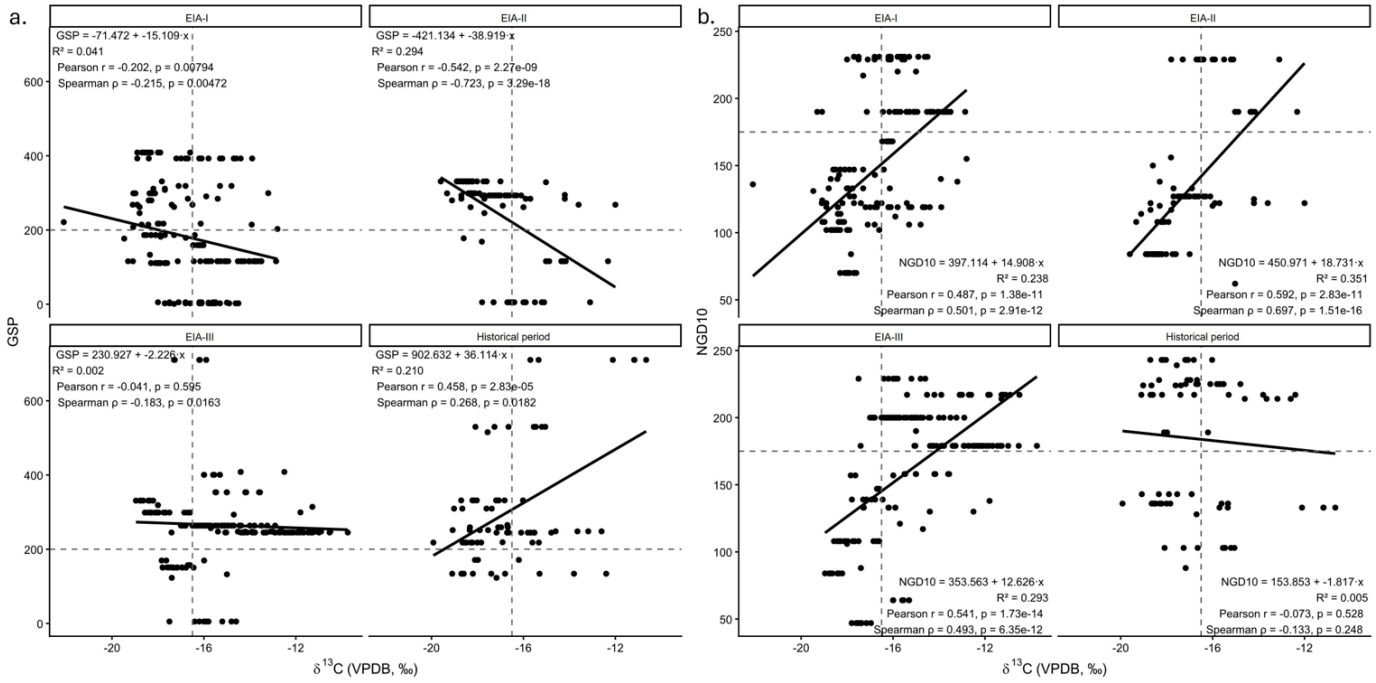


Figure 7

Relationships between δ¹³C values and GSP (a) and NGD10 (b); (a) Relationships between δ¹³C values and accumulated precipitation during the growing season (GSP). Linear regression lines and correlation statistics are shown. A negative relationship between average δ¹³C and GSP indicates that millet consumption increases under drier condition in the Early Iron Age I, II and III (EIA-I, II and III). In contrast, the historical period exhibits the opposite pattern.(b) Relationships between δ¹³C values and the number of growing degree days above 10 °C (NGD10). Solid lines represent linear regression fits. Pearson (r) and Spearman (ρ) correlation coefficients and corresponding p values are shown in each panel. The results indicate a positive correlation between average δ¹³C and NGD10, suggesting increased reliance on millet under lower growing-season heat availability in the Early Iron Age I, II and III (EIA-I, II and III). This trend is reversed during the historical period. Resource of data also refers to Fig. 6

Supplementary Files

This is a list of supplementary files associated with this preprint. Click to download.

- CNisotopesdatasets.xlsx
- RadiocarbonprogramandRcoding.docx
- Testingdetails.docx